PHYSICAL REVIEW B **89**, 134311 (2014)

Dynamics of the Bose-Hubbard chain for weak interactions

Martin L. R. Fürst,[1,2,*] Christian B. Mendl,[2,†] and Herbert Spohn[2,3,‡]

[1]*Excellence Cluster Universe, Technische Universität München, Boltzmannstraße 2, 85748 Garching bei München, Germany*

[2]*Mathematics Department, Technische Universität München, Boltzmannstraße 3, 85748 Garching bei München, Germany*

[3]*Physics Department, Technische Universität München, James-Franck-Straße 1, 85748 Garching bei München, Germany*

(Received 23 December 2013; published 30 April 2014)

We study the Boltzmann transport equation for the Bose-Hubbard chain in the kinetic regime. The time-dependent Wigner function is matrix-valued with odd dimension due to integer spin. For nearest neighbor hopping only, there are infinitely many additional conservation laws and nonthermal stationary states. Adding longer-range hopping amplitudes entails exclusively thermal equilibrium states. Especially for small next-nearest neighbor hopping amplitudes, we observe prethermalization with two time scales, which can be related to the relative strength of the nearest and next-nearest hopping. We provide a derivation of the Boltzmann equation based on the Hubbard Hamiltonian, including general interactions beyond on-site, and illustrate the results by numerical simulations.

DOI: 10.1103/PhysRevB.89.134311 PACS number(s): 05.30.Jp, 67.10.Fj

I. INTRODUCTION

In recent years, Bose-Hubbard models have been realized in experiments using ultracold bosonic atoms in optical lattices [1,2]. These experiments facilitate the study of many-body effects like phase transitions from a superfluid to a Mott insulator [3] and the (de-)coherence dynamics induced by the Hubbard model [4–6]. Nevertheless, the out-of-equilibrium dynamics, convergence to equilibrium and the dynamics after a sudden quench remain topics of active research [7–9].

In this contribution, we study the dynamics of the integer spin Bose-Hubbard chain in the *weakly interacting* ("superfluid") regime, as described by kinetic theory. Our formalism allows for general hopping amplitudes (nearest neighbor, next-nearest neighbor, etc.) and weak interactions beyond on-site, see Sec. III. In previous contributions [10–13], we studied the Fermi-Hubbard model. In case of on-site potential and nearest neighbor hopping, the Fermi-Hubbard Hamiltonian is integrable and has an infinite number of conservation laws. In Ref. [11], we discovered that this integrable structure is still visible on the kinetic level by having many nonthermal stationary states. On the other hand, while the general spin Bose-Hubbard Hamiltonian with the same couplings is apparently not integrable, the Boltzmann transport equation still has an infinite number of conservation laws, as to be discussed in Sec. IV. Hence the link between microscopic integrability and infinite number of conservation laws on the kinetic level is less stringent than anticipated in Ref. [11].

For all Hubbard models, the additional conservation laws disappear when turning on hopping beyond nearest neighbor: all stationary states are thermal (Bose-Einstein, resp. Fermi-Dirac) distributions, see Sec. V. For small next-nearest neighbor hopping amplitudes, we observe prethermalization [14–16] with a definite signature. The system quickly converges to the nonthermal quasistationary state dictated by nearest neighbor hops only. The next-nearest neighbor hops slightly modify the collision rates, which in the long run establishes thermalization. In this sense, the next-nearest neighbor hopping can be regarded as perturbation, which establishes the additional slow time scale.

Our framework allows for inverted populations, thermalizing to a Bose-Einstein equilibrium state with formally negative temperature $1/\beta$, as recently realized experimentally [17]. We will illustrate by a model calculation in Sec. VI that shifting the momentum of the initial Wigner state, $k \to k + \frac{1}{2}$, flips the sign of β of the ($t \to \infty$) stationary thermal state. Interestingly, this thermal state is (in general) not simply a shifted copy of the thermal state matching the initial state before the shift.

While outside the scope of our contribution, we have to point out one important feature of the kinetic equation for the Bose-Hubbard model. Physically, for dimension $d \geqslant 3$ and at sufficiently high density, there will be a superfluid phase, a property that is still reflected at the kinetic level, see Ref. [18] and references therein. In the spatially homogeneous setting, if the initial Wigner function is smooth but of a sufficiently high density, after some finite time span, a δ function will be formed at momentum $k = 0$. The kinetic equation has then to be augmented by coupling it to an evolution equation for the superfluid density. For $d = 1$, as discussed here, to each initial Wigner function there is a uniquely determined stationary Bose-Einstein distribution. For $d \geqslant 3$, this property holds only if the superfluid density is included.

II. BOSE-HUBBARD HAMILTONIAN

We first write down the Hamiltonian of the Bose-Hubbard chain under study. The bosons are described by an integer spin-n field on $\mathbb{Z}$ with creation and annihilation operators satisfying the commutation relations:

$$[a_\sigma(x)^*, a_\tau(y)] = \delta_{xy}\delta_{\sigma\tau}, \tag{1}$$

$$[a_\sigma(x), a_\tau(y)] = 0, \tag{2}$$

$$[a_\sigma(x)^*, a_\tau(y)^*] = 0 \tag{3}$$

*mfuerst@ma.tum.de

†mendl@ma.tum.de

‡spohn@ma.tum.de

for $x,y \in \mathbb{Z}, \sigma,\tau \in \{-n,\dots,n\}$, and $[A,B] = AB - BA$. The Hamiltonian reads

$$\begin{aligned} H &= H_0 + \lambda H_1 \\ &= \sum_{x,y\in\mathbb{Z}} \alpha(x-y)\, a(x)^* \cdot a(y) \\ &\quad + \frac{\lambda}{2} \sum_{x,y\in\mathbb{Z}} V(x-y)(a(x)^* \cdot a(x))(a(y)^* \cdot a(y)). \end{aligned} \tag{4}$$

Here, α is the hopping amplitude, which satisfies $\alpha(x) = \alpha(x)^*$ and $\alpha(x) = \alpha(-x)$. The dispersion relation $\omega(k)$ is precisely its Fourier transform: $\omega(k) = \hat{\alpha}(k)$. In Eq. (4), $a(x)^* \cdot a(x) = \sum_\sigma a_\sigma(x)^* a_\sigma(x)$, and $0 < \lambda \ll 1$ is the strength of the interaction. The pair potential λV consists of a scalar-valued nonnegative function $V : \mathbb{Z} \to \mathbb{R}$, which satisfies $V(x) = V(-x)$. For the on-site case, $V(x) = \delta_{x,0}$, the Fourier transform is constant, $\hat{V}(k) \equiv 1$.

We use the following convention for the Fourier transform:

$$\hat{f}(k) = \sum_{x\in\mathbb{Z}} f(x)\, e^{-2\pi i\, k\, x}, \tag{5}$$

such that the first Brillouin zone is the interval $\mathbb{T} = [-\frac{1}{2},\frac{1}{2}]$ with periodic boundary conditions. H can be written in Fourier space as

$$\begin{aligned} H &= \int_{\mathbb{T}} dk\, \omega(k)\, (\hat{a}(k)^* \cdot \hat{a}(k)) \\ &\quad + \frac{\lambda}{2} \int_{\mathbb{T}^4} d^4\boldsymbol{k}\, \delta(\underline{k})\, \hat{V}(k_1 - k_2) \\ &\quad \times (\hat{a}(k_1)^* \cdot \hat{a}(k_2))(\hat{a}(k_3)^* \cdot \hat{a}(k_4)) \end{aligned} \tag{6}$$

with $\underline{k} = k_1 - k_2 + k_3 - k_4 \mod 1$ and $d^4\boldsymbol{k} = dk_1\, dk_2\, dk_3\, dk_4$. Note that the convention for $\underline{k}$ differs from Refs. [10,11] by an interchange of $k_2 \leftrightarrow k_3$, for consistency with the derivation in Appendix B.

In this contribution, we will study a prototypical model with nearest neighbor hopping and an additional next-nearest neighbor hopping term with tunable weight η. The corresponding dispersion relation reads

$$\omega_\eta(k) = 1 - \cos(2\pi k) - \eta \cos(4\pi k), \tag{7}$$

and the pure nearest neighbor hopping case corresponds to $\eta = 0$.

III. BOLTZMANN-HUBBARD EQUATION

We will derive the kinetic Boltzmann equation in Appendix B, in analogy to the fermionic case [12]. The central object is the two-point function $W(k,t)$ defined by the relation

$$\langle \hat{a}_\sigma(k,t)^*\, \hat{a}_\tau(\tilde{k},t) \rangle = \delta(k - \tilde{k})\, W(k,t)_{\sigma\tau}. \tag{8}$$

For each $k \in \mathbb{T}$, $W(k,t)$ is a $(2n+1) \times (2n+1)$ positive semidefinite matrix. The resulting Boltzmann equation reads

$$\frac{\partial}{\partial t} W(k,t) = \mathcal{C}_\text{c}[W](k,t) + \mathcal{C}_\text{d}[W](k,t) \equiv \mathcal{C}[W](k,t), \tag{9}$$

with the first term of Vlasov type,

$$\mathcal{C}_\text{c}[W](k,t) = -i\, [H_\text{eff}(k,t), W(k,t)], \tag{10}$$

where the effective Hamiltonian $H_\text{eff}(k,t)$ is a $(2n+1) \times (2n+1)$ matrix which itself depends on W. More explicitly,

$$\begin{aligned} H_{\text{eff},1} &= \int_{\mathbb{T}^3} dk_2 dk_3 dk_4\, \delta(\underline{k})\, \mathcal{P}\left(\frac{1}{\underline{\omega}}\right) \\ &\quad \times \big(\hat{V}_{23}\hat{V}_{34}(W_2W_3 + W_3W_2 - W_2W_4 + W_3) \\ &\quad + \hat{V}_{34}^2 \operatorname{tr}[W_3 - W_4]W_2\big). \end{aligned} \tag{11}$$

Here and later on, we use the shorthand $\tilde{W} = 1 + W$, $W_1 = W(k_1,t)$, $H_{\text{eff},1} = H_\text{eff}(k_1,t)$, $\underline{\omega} = \omega(k_1) - \omega(k_2) + \omega(k_3) - \omega(k_4)$, and $\hat{V}_{ij} = \hat{V}(k_i - k_j)$. Note that $\hat{V}_{34} = \hat{V}_{12}$ in Eq. (11) due to $k_1 - k_2 = k_4 - k_3$ and the symmetry of $\hat{V}$.

The collision term $\mathcal{C}_\text{d}$ can be written as

$$\mathcal{C}_\text{d}[W]_1 = \pi \int_{\mathbb{T}^3} dk_2 dk_3 dk_4\, \delta(\underline{k})\, \delta(\underline{\omega})(\mathcal{A}[W]_{1234} + \mathcal{A}[W]_{1234}^*), \tag{12}$$

where the index 1234 means that the matrix $\mathcal{A}[W]$ depends on k_1, k_2, k_3, and k_4. Explicitly,

$$\begin{aligned} \mathcal{A}[W]_{1234} &= \hat{V}_{23}\hat{V}_{34}\, W_4\tilde{W}_3W_2 + \hat{V}_{34}^2\, W_4 \operatorname{tr}[W_2\tilde{W}_3] \\ &\quad + W_1\big(\hat{V}_{23}\hat{V}_{34}(W_2\tilde{W}_4 - W_3\tilde{W}_4 - W_2\tilde{W}_3) \\ &\quad + \hat{V}_{34}^2(\tilde{W}_4 \operatorname{tr}[W_2 - W_3] - \operatorname{tr}[W_2\tilde{W}_3])\big). \end{aligned} \tag{13}$$

The gain term, consisting of the first two summands (plus their conjugate-transposes), is always positive semidefinite as proved in Appendix A. Hence, if W_1 has an hypothetical zero eigenvalue, then the term $W_1(\dots)$ projected onto the corresponding eigenvector vanishes and the gain term pushes the eigenvalue back to be positive. The δ function of the collision term contains both normal processes and umklapp processes for which $k_1 - k_2 + k_3 - k_4 = \pm 1$.

Using $k_2 \leftrightarrow k_4$, the integrand in Eq. (12) admits the reformulation

$$\mathcal{A}[W]_{1234} + \mathcal{A}[W]_{1234}^* = \mathcal{A}_\text{quad}[W]_{1234} + \mathcal{A}_\text{tr}[W]_{1234} \tag{14}$$

with

$$\begin{aligned} \mathcal{A}_\text{quad}[W]_{1234} &= \hat{V}_{23}\hat{V}_{34}(\tilde{W}_1W_2\tilde{W}_3W_4 + W_4\tilde{W}_3W_2\tilde{W}_1 \\ &\quad - W_1\tilde{W}_2W_3\tilde{W}_4 - \tilde{W}_4W_3\tilde{W}_2W_1) \end{aligned} \tag{15}$$

and

$$\begin{aligned} \mathcal{A}_\text{tr}[W]_{1234} &= \hat{V}_{34}^2((\tilde{W}_1W_2 + W_2\tilde{W}_1)\operatorname{tr}[\tilde{W}_3W_4] \\ &\quad - (W_1\tilde{W}_2 + \tilde{W}_2W_1)\operatorname{tr}[W_3\tilde{W}_4]). \end{aligned} \tag{16}$$

As a remark, the conservative collision operator $\mathcal{C}_\text{c}$ can be written as

$$\begin{aligned} \mathcal{C}_\text{c}[W](k,t) &= -i \int_{\mathbb{T}^3} dk_2 dk_3 dk_4 \delta(\underline{k})\, \mathcal{P}\left(\frac{1}{\underline{\omega}}\right) \\ &\quad \times (\mathcal{A}[W]_{1234} - \mathcal{A}[W]_{1234}^*). \end{aligned} \tag{17}$$

IV. GENERAL PROPERTIES OF THE HUBBARD KINETIC EQUATION

The SU$(2n+1)$ invariance of H is reflected by

$$\mathcal{C}[U^*WU] = U^*\mathcal{C}[W]U \tag{18}$$

for all $U \in \mathrm{SU}(2n+1)$. Hence, if $W(k,t)$ is a solution to the Boltzmann equation (9), so is $U^* W(k,t) U$. Analogous to the Fermi case, hermiticity and positivity, $W(t) \geqslant 0$, is propagated in time. Positivity is enforced by the "gain term" in Eq. (13).

In general, spin

$$\int_{\mathbb{T}} dk\, W(k,t) \tag{19}$$

and energy

$$\int_{\mathbb{T}} dk\, \omega(k)\, \mathrm{tr}[W(k,t)] \tag{20}$$

are conserved. As discussed in Refs. [10,11], additional conservation laws emerge depending on the dispersion relation $\omega(k)$. Namely, for the nearest neighbor hopping model, $\eta = 0$ in Eq. (7), the function

$$h(k,t) = \mathrm{tr}[W(k,t)] - \mathrm{tr}\big[W\big(\tfrac{1}{2}-k,t\big)\big] \tag{21}$$

remains constant in time (pointwise for each $k \in \mathbb{T}$). Using similar arguments as in the fermionic case, the conservation laws follow by an appropriate interchange of the integration variables $k_1,\ldots,k_4$.

To prove the H theorem, we first recall the definition of the entropy for bosons (log here and subsequently is the natural logarithm):

$$S[W] = \int_{\mathbb{T}} dk_1 (\mathrm{tr}[\tilde{W}_1 \log \tilde{W}_1] - \mathrm{tr}[W_1 \log W_1]). \tag{22}$$

Hence the entropy production is given by

$$\sigma[W] = \frac{d}{dt} S[W] = \int_{\mathbb{T}} dk_1\, \mathrm{tr}[(\log \tilde{W}_1 - \log W_1)\mathcal{C}[W]_1]. \tag{23}$$

The H-theorem states that

$$\sigma[W] \geqslant 0 \quad \text{for all positive semidefinite } W. \tag{24}$$

To prove (24), we start from the eigendecomposition (at fixed t)

$$W(k) = \sum_{\sigma} \lambda_\sigma(k) P_\sigma(k) \tag{25}$$

with eigenvalues $\lambda_\sigma(k) \geqslant 0$ and orthogonal eigenprojections $P_\sigma(k) = |k,\sigma\rangle\langle k,\sigma|$, such that $\langle k,\sigma|k,\sigma'\rangle = \delta_{\sigma\sigma'}$. As before, we use the notation $P_j = P_{\sigma_j}(k_j)$, $\lambda_j = \lambda_{\sigma_j}(k_j)$ and $\sum_{\boldsymbol{\sigma}} = \sum_{\sigma_1,\sigma_2,\sigma_3,\sigma_4}$. Inserting (25) into (23) and using the representation in Eqs. (15) and (16) as well as the interchangeability $k_2 \leftrightarrow k_4$, one obtains

$$\begin{aligned}
\sigma[W] &= \pi \int_{\mathbb{T}^4} d^4\boldsymbol{k}\, \delta(\underline{k})\delta(\underline{\omega}) \\
&\quad \times \sum_{\boldsymbol{\sigma}} (\log \tilde{\lambda}_1 - \log \lambda_1)(\tilde{\lambda}_1\lambda_2\tilde{\lambda}_3\lambda_4 - \lambda_1\tilde{\lambda}_2\lambda_3\tilde{\lambda}_4) \\
&\quad \times \big(\hat{V}_{34}^2\, \mathrm{tr}[P_1P_2]\mathrm{tr}[P_3P_4] + \hat{V}_{23}^2\, \mathrm{tr}[P_1P_4]\mathrm{tr}[P_2P_3] \\
&\qquad + \hat{V}_{23}\hat{V}_{34}\, \mathrm{tr}[P_1P_2P_3P_4] + \hat{V}_{23}\hat{V}_{34}\, \mathrm{tr}[P_4P_3P_2P_1]\big) \\
&= \pi \int_{\mathbb{T}^4} d^4\boldsymbol{k}\, \delta(\underline{k})\delta(\underline{\omega}) \sum_{\boldsymbol{\sigma}} (\tilde{\lambda}_1\lambda_2\tilde{\lambda}_3\lambda_4 - \lambda_1\tilde{\lambda}_2\lambda_3\tilde{\lambda}_4) \\
&\quad \times \log(\tilde{\lambda}_1/\lambda_1)\, |\hat{V}_{34}\, \langle k_1,\sigma_1|k_2,\sigma_2\rangle\langle k_3,\sigma_3|k_4,\sigma_4\rangle \\
&\qquad + \hat{V}_{23}\, \langle k_1,\sigma_1|k_4,\sigma_4\rangle\langle k_3,\sigma_3|k_2,\sigma_2\rangle|^2.
\end{aligned} \tag{26}$$

Interchanging $1 \leftrightarrow 3$, $2 \leftrightarrow 4$, and $(1,3) \leftrightarrow (2,4)$ and using $\hat{V}_{34} = \hat{V}_{12}$, $\hat{V}_{23} = \hat{V}_{14}$ due to $\delta(\underline{k})$, one arrives at

$$\begin{aligned}
\sigma[W] &= \frac{\pi}{4} \int_{\mathbb{T}^4} d^4\boldsymbol{k}\, \delta(\underline{k})\delta(\underline{\omega}) \\
&\quad \times \sum_{\boldsymbol{\sigma}} (\tilde{\lambda}_1\lambda_2\tilde{\lambda}_3\lambda_4 - \lambda_1\tilde{\lambda}_2\lambda_3\tilde{\lambda}_4) \log\left(\frac{\tilde{\lambda}_1\lambda_2\tilde{\lambda}_3\lambda_4}{\lambda_1\tilde{\lambda}_2\lambda_3\tilde{\lambda}_4}\right) \\
&\quad \times |\hat{V}_{34}\, \langle k_1,\sigma_1|k_2,\sigma_2\rangle\langle k_3,\sigma_3|k_4,\sigma_4\rangle \\
&\qquad + \hat{V}_{23}\, \langle k_1,\sigma_1|k_4,\sigma_4\rangle\langle k_3,\sigma_3|k_2,\sigma_2\rangle|^2.
\end{aligned} \tag{27}$$

The last expression is $\geqslant 0$ since $(x-y)\log(x/y) \geqslant 0$.

From the form of (27) one concludes that the stationary states (discussed below) do not depend on the potential, as long as $\hat{V}(k)$ stays nonzero for all $k \in \mathbb{T}$.

V. STATIONARY SOLUTIONS

The kinematically allowed collisions depend only on the dispersion $\omega(k)$ and are discussed already in Ref. [11]. The initial state determines a special, k-independent basis $|\sigma\rangle$ through

$$\int_{\mathbb{T}} dk\, W(k) = \sum_{\sigma} \varepsilon_\sigma\, |\sigma\rangle\langle\sigma|. \tag{28}$$

By the spin conservation (19) this basis is preserved in time. Thus it is natural to expand $W(k,t)$ in this special basis.

For long times, we expect that $W(k,t)$ will become diagonal in the conserved spin basis, analogous to the fermionic case [10,11]. Without the additional conservation laws in Eq. (21), $W(k,t)$ will converge to a thermal Bose-Einstein distribution

$$W_{\mathrm{th}}(k) = \sum_{\sigma} \big(e^{\beta(\omega(k)-\mu_\sigma)} - 1\big)^{-1} |\sigma\rangle\langle\sigma|, \tag{29}$$

with temperature $1/\beta$ and chemical potentials μ_σ, precisely in accordance with the conserved spin and energy. For the nearest neighbor case with conserved $h(k,t)$, the stationary solutions should have the same structure as in Eq. (29), but with $\omega(k)$ replaced by a more general function f. One obtains

$$W_{\mathrm{st}}(k) = \sum_{\sigma} \lambda_\sigma(k)\, |\sigma\rangle\langle\sigma|, \quad \lambda_\sigma(k) = (e^{f(k)-a_\sigma} - 1)^{-1}, \tag{30}$$

where f is a real-valued, 1-periodic function satisfying $f(k) = -f(\frac{1}{2}-k)$ and $f(k) - a_\sigma > 0$ for all k, σ.

Assuming that the initial W converges to a stationary state of the form (30), it must hold that

$$h(k) = \sum_{\sigma} ((e^{f(k)-a_\sigma} - 1)^{-1} - (e^{-f(k)-a_\sigma} - 1)^{-1}). \tag{31}$$

The spin-conservation law requires that the eigenvalues ε_σ in Eq. (28) are equal to

$$\varepsilon_\sigma = \int_{\mathbb{T}} dk\, (e^{f(k)-a_\sigma} - 1)^{-1}. \tag{32}$$

We claim that (31) and (32) uniquely determine f and a_σ, or more specifically, that the map between

$$\mathrm{tr}[W(k)] - \mathrm{tr}\big[W\big(\tfrac{1}{2}-k\big)\big], \quad |k| \leqslant \tfrac{1}{4}, \quad \varepsilon_\sigma \geqslant 0 \text{ for all } \sigma \tag{33}$$

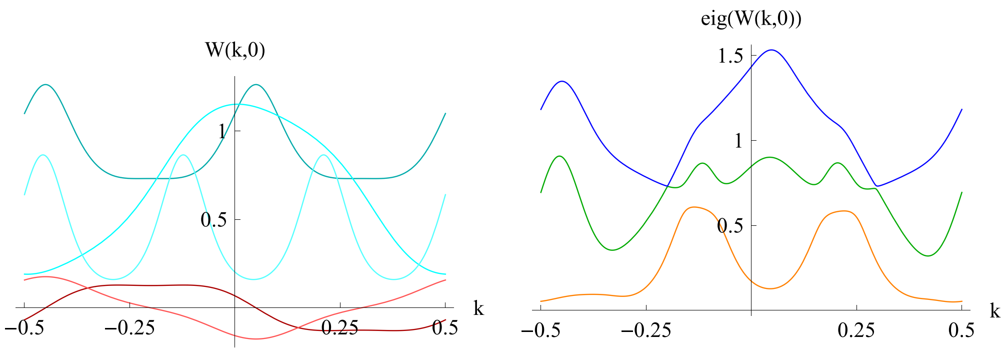

(a) matrix entries (b) eigenvalues

FIG. 1. (Color online) The initial state $W(k,0)$ used for the simulations. (a) The cyan (upper) curves show the real diagonal entries, and the darker and lighter red curves the real and imaginary parts of the off-diagonal $|0\rangle\langle\downarrow|$ entry, respectively. For visual clarity, the remaining off-diagonal entries are omitted in the plot. (b) Eigenvalues of $W(k,0)$. Note the crossing (at negative k) and avoided crossing (at positive k) of the upper two curves.

and

$$\{f(k),a_\sigma\} \text{ with } f(k) = -f\left(\tfrac{1}{2}-k\right) \quad \text{for } |k| \leqslant \tfrac{1}{4}, \qquad f(k) - a_\sigma > 0 \quad \text{for all } k,\sigma \tag{34}$$

is one-to-one. In particular, to a given W one can associate a unique W_{st} of the form (30).

Proof of the bijective mapping. By a short calculation, (31) can be written as

$$h(k) = \sum_\sigma \frac{-\sinh f(k)}{\cosh a_\sigma - \cosh f(k)} \tag{35}$$

and (32) as

$$\varepsilon_\sigma = \int_{\mathrm{I}} dk \left(\frac{-\sinh a_\sigma}{\cosh a_\sigma - \cosh f(k)} - 1 \right) \tag{36}$$

with interval of integration $\mathrm{I} = [-\frac{1}{4},\frac{1}{4}]$. We define a generalized "free energy" through

$$H(f,a_\sigma) = \int_{\mathrm{I}} dk \sum_\sigma -\log\big(\cosh a_\sigma - \cosh f(k)\big). \tag{37}$$

The map $(f,a_\sigma) \mapsto H$ is strictly convex: namely, H is an integral and sum of functions

$$(f,a) \mapsto -\log(\cosh a - \cosh f), \quad |f| < |a|, \tag{38}$$

which are strictly convex since the eigenvalues of the Hessian matrix are $\cosh(a \pm f) - 1 > 0$. Furthermore,

$$\frac{\partial}{\partial a_\sigma} H = \int_{\mathrm{I}} dk \frac{-\sinh a_\sigma}{\cosh a_\sigma - \cosh f(k)} = \varepsilon_\sigma - \frac{1}{2} \tag{39}$$

and

$$\frac{\delta H}{\delta f(k)} = \sum_\sigma \frac{\sinh f(k)}{\cosh a_\sigma - \cosh f(k)} = -h(k). \tag{40}$$

Thus the map from above can be viewed as Legendre transform from the first set (33) to the second set of variables (34). Since H is convex, the map is one-to-one. ■

VI. SIMULATION

The details of the numerical implementation and mollification of the collision operator have been adapted from [11] to the bosonic case. Here, we report simulation results. For better comparison, we start always from the same initial state and modify the parameters of the evolution equation.

A. Initial Wigner state

We fix the initial condition $W(k,0)$ as illustrated in Fig. 1. The cyan lines in Fig. 1(a) represent the real diagonals, and the dark and light red functions the real and imaginary parts of the off-diagonal $|0\rangle\langle\downarrow|$ entry, respectively. The eigenvalues of $W(k,0)$ in Fig. 1(b) are non-negative for each $k \in \mathbb{T}$, as required, and $W(k,0)$ is continuous on $\mathbb{T}$. Note that the eigenvalues can exceed 1, different from the Fermi case. One observes that the eigenvalue crossing evolves to an avoided crossing during the simulation. For reference, the analytical formulas of the matrix entries are provided in Appendix D.

B. Stationary states

One can obtain the stationary state corresponding to the initial $W(k,0)$ via the conservation laws Eqs. (19)–(21), as shown in Sec. V. Different dispersion relations lead to different stationary states, which are illustrated in Fig. 2 for the nearest and next-nearest neighbor hopping models. The next-nearest neighbor cases result in thermal Bose-Einstein distributions, while the nearest neighbor case results in a nonthermal stationary state of the form (30), see Fig. 2(a). The corresponding f function is shown in Fig. 2(b).

C. Exponential convergence and prethermalization

The next-nearest neighbor model with small $\eta = \frac{1}{50}$ serves as illustration of the prethermalization effect. In our context, the initial Wigner state converges quickly to a quasistationary state close to the nonthermal stationary state in Fig. 2(a) (nearest neighbor model with $\eta = 0$), and then thermalizes slowly to the equilibrium state in Fig. 2(c). The entropy increase [shown in Fig. 3(a)] quantifies this dynamical picture: the entropy quickly reaches the entropy of the stationary nearest neighbor state (dashed black curve), and then further increases towards the actual thermal equilibrium state, with an exponential decay rate of 0.136. For comparison, the decay rate to the nonthermal stationary state for $\eta = 0$ is 13.47.

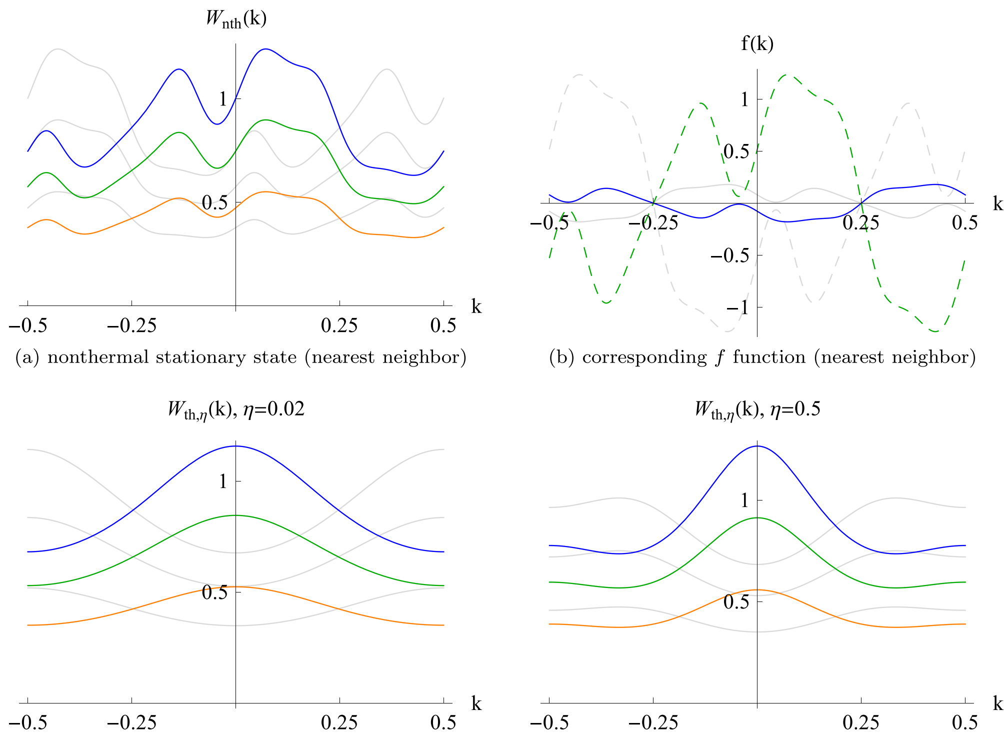

(a) nonthermal stationary state (nearest neighbor)

(b) corresponding f function (nearest neighbor)

(c) thermal equilibrium state (next-nearest neighbor hopping, with $\eta = \frac{1}{50}$)

(d) thermal equilibrium state (next-nearest neighbor hopping, with $\eta = \frac{1}{2}$)

FIG. 2. (Color online) Diagonal matrix entries (colored curves) of the stationary ($t \to \infty$) states corresponding to the initial $W(k,0)$ in Fig. 1, for the nearest neighbor hopping model (a) and the next-nearest neighbor model with $\eta = \frac{1}{50}$ (c) and $\eta = \frac{1}{2}$ (d). The off-diagonal matrix entries are zero. Apparently, the final state sensitively depends on the dispersion relation $\omega(k)$. The additional conservation laws in the nearest neighbor case lead to a nonthermal stationary state. (b) The f function (solid blue) and conserved $\mathrm{tr}[W(k)] - \mathrm{tr}[W(\frac{1}{2} - k)]$ (dashed green) for the nearest neighbor hopping model, which determines the nonthermal stationary state in (a). The faint gray curves show the corresponding entries when shifting the initial state $k \to k + \frac{1}{2}$, resulting in negative temperatures of the thermal stationary states. Note that the gray curves in (a) are exact shifted duplicates, which holds not true for the next-nearest neighbor models in (c) and (d). As discussed after Eq. (27), the stationary states do not depend on the potential $\hat{V}(k)$.

An analytical approach in terms of the vanishing off-diagonal entries follows the same lines as in Ref. [11], and is illustrated in Fig. 3(b).

D. Population inversion (negative temperature)

States with formally negative temperatures ($\beta < 0$) have recently attracted interest [17,19]. In our context, first observe

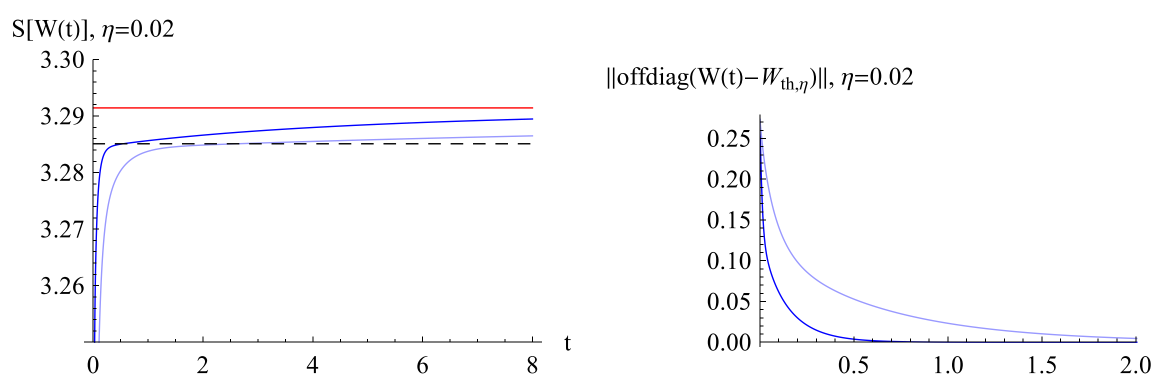

(a) entropy increase

(b) convergence of the off-diagonal entries

FIG. 3. (Color online) (a) Entropy increase for the next-nearest neighbor model with small $\eta = \frac{1}{50}$ (dark blue curve). The red curve shows the entropy of the corresponding equilibrium state, and the dashed black curve the entropy of the stationary nearest neighbor state. The entropy increases quickly up to $t \simeq 0.5$, where it reaches the dashed curve ("fast motion"). Afterwards, it slowly approaches the actual thermal equilibrium value ("slow motion"). (b) Exponential convergence of the off-diagonal entries. The dynamic matches the "fast motion" in (a) quite well, i.e., the off-diagonal entries (almost) reach zero within the "fast motion" period. For visual clarity, the time axis in (b) is shorter than in (a). To demonstrate the effect of the potential, the faint blue curves show the results for a calculation with the potential in Fig. 5 instead of the uniform $\hat{V}(k) \equiv 1$.

that the exponential term of the Bose-Einstein distribution

$$(e^{\beta(\omega(k)-\mu_\sigma)} - 1)^{-1} \tag{41}$$

is invariant under $\beta \to -\beta$ when simultaneously changing the sign of $\omega(k) - \mu_\sigma$. As argued in Ref. [19], a sign flip of the *nearest neighbor* dispersion (up to an arbitrary offset) is accomplished by shifting the momentum $k \to k + \frac{1}{2}$. In terms of the f function in Eq. (30), the shift of momentum is equivalent to a point reflection at the origin since $f(k + \frac{1}{2}) = -f(-k)$. However, for the next-nearest neighbor models, the sign-flip property of the dispersion holds not exactly true due to the additional $\eta\cos(4\pi k)$ term, which is invariant under $k \to k + \frac{1}{2}$.

Nevertheless, it turns out that simply shifting the initial state in Fig. 1 by $k \to k + \frac{1}{2}$ suffices to obtain thermal equilibrium states with negative temperature. The states resulting from the initial shift are shown as faint gray curves in Fig. 2. Note that the thermal gray curves attain their maximum at (or close to) the boundary of the Brillouin zone, while positive temperature states have their maximum at $k = 0$. As expected, for the nearest neighbor model the f function is reflected about the origin and the gray curves in (a) are shifted copies of the original colored curves, whereas for the next-nearest neighbor model this does no longer hold since $\omega_\eta(k + \frac{1}{2}) \neq -\omega_\eta(k) + c$ for nonzero η. The inverse temperature β of the thermal states is shown in the following table. Note that the shift also changes the absolute value:

	$\eta = 0.02$	$\eta = 0.5$
β of original $W(k,0)$	0.1403	0.1228
β of shifted $W(k + \frac{1}{2},0)$	−0.1394	−0.09507

E. Effect of the potential

The three eigenvalues of a spin-1 Wigner state $W(k,t)$ define a point in $\mathbb{R}^3$. We thus obtain for each t a spectral curve of eigenvalues as k traverses the Brillouin zone $\mathbb{T}$, as visualized in Fig. 4 for the next-nearest neighbor model with $\eta = \frac{1}{2}$.

Comparing a simulation using the standard on-site potential $\hat{V}(k) \equiv 1$ with a k-dependent potential $\hat{V}(k) = 1/(2 - \cos(2\pi k))$, one notices that the convergence for the k-dependent potential is slower as compared to the on-site case; this observation can be confirmed quantitatively: the exponential decay rate in Hilbert-Schmidt norm is 0.67 and 0.25, respectively. The potential is visualized in Fig. 5.

The kinematically allowed collisions $\delta(\underline{k})\,\delta(\underline{\omega})$ define the collision manifold, a subset of $\mathbb{T}^4$. Specifically for the next-nearest neighbor model with $\eta = \frac{1}{2}$, it consists of the γ_1, γ_2, γ_{diag}, and γ_{ellip} manifolds as discussed in Ref. [11]. Figure 6 shows the latter two, with color encoding the eigenvalues of $\mathcal{A}_{\text{quad}}$ on the left and $\mathcal{A}_{\text{tr}}$ on the right (for the initial state $W(k,0)$ and $\hat{V}(k) \equiv 1$). Considering the effect of the potential in Fig. 5, let us briefly elaborate on the weighting of the collisions by the $\hat{V}$ prefactors of the $\mathcal{A}_{\text{quad}}$ and $\mathcal{A}_{\text{tr}}$ integrands. Since $\hat{V}(k)$ attains its maximum at $k = 0$, the scale factor $\hat{V}(k_2 - k_3)\hat{V}(k_3 - k_4)$ is largest when the momenta $k_1, \ldots, k_4$ are all equal. Concerning $\hat{V}(k_3 - k_4)^2$, the hyperplane $k_3 = k_4$ (or equivalently $k_1 = k_2$) contributes the most.

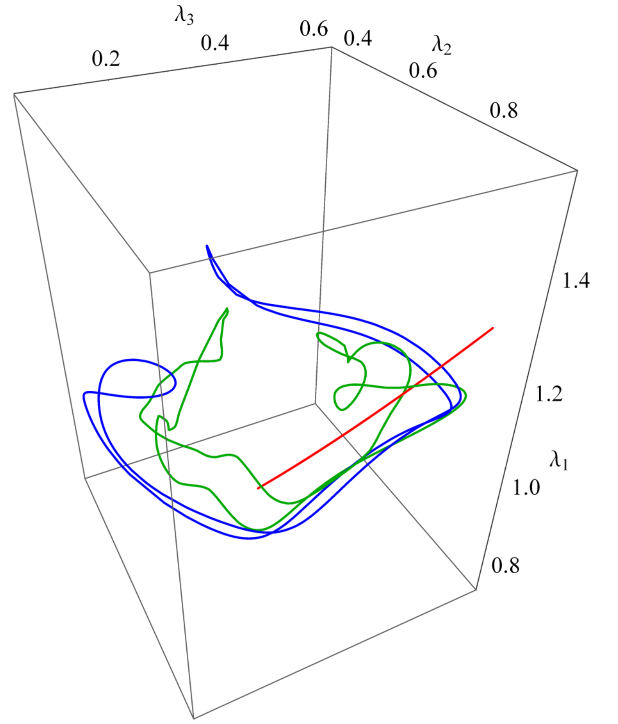

FIG. 4. (Color online) Time evolution of the eigenvalues of $W(k,t)$ for the next-nearest neighbor model with $\eta = \frac{1}{2}$ and the k-dependent potential in Fig. 5. Each curve shows the three eigenvalues of $W(k,t)$ as k traverses the Brillouin zone $\mathbb{T}$, for fixed t. The blue and green colors correspond to $t = 0$ [also see Fig. 1(b)] and $t = 1/16$, respectively. The red curve corresponds to the final thermal equilibrium state [illustrated in Fig. 2(b)].

VII. CONCLUSIONS

On the kinetic level, the dynamics of bosons and fermions in one dimension is qualitatively similar: additional conservation laws and nonthermal stationary states exist for pure nearest neighbor hopping. These additional conservation laws disappear when turning on longer range hopping terms, and all stationary states become thermal equilibrium states.

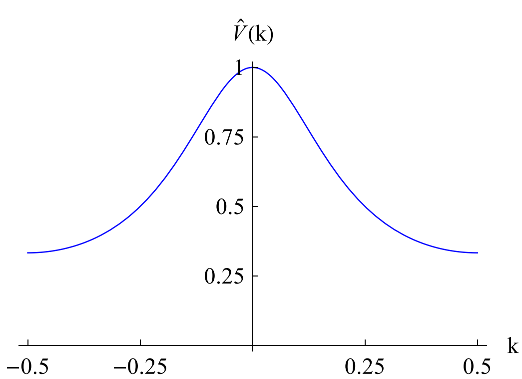

FIG. 5. (Color online) The k-dependent potential $\hat{V}(k) = 1/(2 - \cos(2\pi k))$ used in the simulation in Fig. 4.

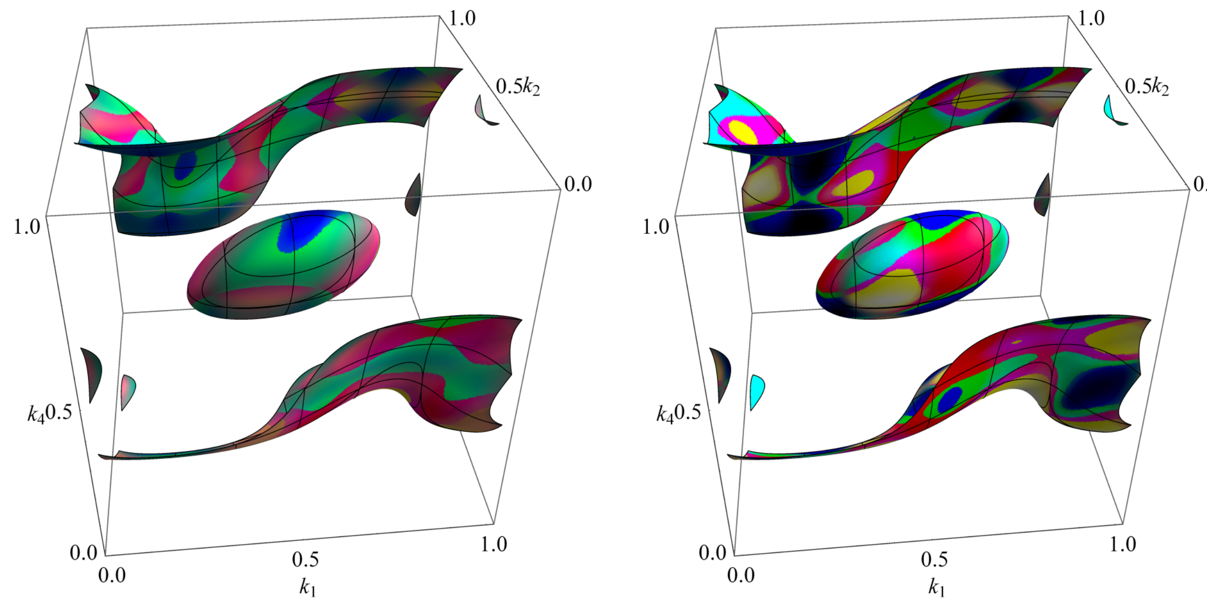

(a) $\mathrm{eig}(\mathcal{A}_{\mathrm{quad}})$ (b) $\mathrm{eig}(\mathcal{A}_{\mathrm{tr}})$

FIG. 6. (Color online) Three-dimensional shape of the γ_{diag} and γ_{ellip} collision manifolds for the next-nearest neighbor model with $\eta = \frac{1}{2}$. Color encodes the eigenvalues of (a) $\mathcal{A}_{\mathrm{quad}}$ and (b) $\mathcal{A}_{\mathrm{tr}}$ in Eqs. (15) and (16) with the $\hat{V}_{ij}$ prefactors set to 1, for the initial state $W(k,0)$. Eigenvalues can be negative, and the zero state corresponds to gray color.

Prethermalization is observed for small next-nearest neighbor hopping, and the hopping amplitude controls the time scale of the slow convergence to thermal equilibrium.

Conversely, the main modifications for bosons include the following: $\tilde{W} = 1 - W$ for fermions is replaced by $\tilde{W} = 1 + W$ for bosons, the Wigner matrix $W(k)$ has dimension $(2n+1) \times (2n+1)$ where $n \in \mathbb{N}_0$ is the spin quantum number, and the Fermi property $0 \leqslant W(k) \leqslant 1$ is relaxed to $0 \leqslant W(k)$ for bosons. Concerning inverted populations, the shift-invariance of the evolution dynamics with respect to $k \to k + \frac{1}{2}$ is broken by the dispersion relation whenever $\omega(k + \frac{1}{2}) \neq -\omega(k) + c$.

APPENDIX A: POSITIVITY

The following lemma ensures positivity of the gain term in Eq. (13), when identifying $x = \hat{V}_{34}$, $y = -\hat{V}_{23}$ and using the interchangeability of the integration variables $k_2 \leftrightarrow k_4$.

Lemma 1. Let $A,B,C \in \mathbb{C}^{d\times d}$ be positive semidefinite and $x,y \in \mathbb{R}$. Then

$$x^2\, A\,\mathrm{tr}[B\,C] + y^2\, C\,\mathrm{tr}[B\,A] - x\,y\,ABC - x\,y\,C\,B\,A \geqslant 0.$$

Proof. By the spectral decomposition of B with non-negative eigenvalues, we can without loss of generality assume that $B = |\psi\rangle\langle\psi|$ for a $\psi \in \mathbb{C}^d$. Now let $\varphi \in \mathbb{C}^d$ be arbitrary, then

$$\begin{aligned}
&\langle\varphi|x^2\, A\,\mathrm{tr}[B\,C] + y^2\, C\,\mathrm{tr}[B\,A] - x\,y\,ABC - x\,y\,C\,B\,A|\varphi\rangle\\
&\quad= x^2\langle\varphi|A|\varphi\rangle\langle\psi|C|\psi\rangle + y^2\langle\varphi|C|\varphi\rangle\langle\psi|A|\psi\rangle\\
&\qquad - x\,y\langle\varphi|A|\psi\rangle\langle\psi|C|\varphi\rangle - x\,y\langle\varphi|C|\psi\rangle\langle\psi|A|\varphi\rangle\\
&\quad\geqslant x^2\langle\varphi|A|\varphi\rangle\langle\psi|C|\psi\rangle + y^2\langle\varphi|C|\varphi\rangle\langle\psi|A|\psi\rangle\\
&\qquad - 2\,|x\,y||\langle\varphi|A|\psi\rangle||\langle\psi|C|\varphi\rangle|.
\end{aligned}$$

Using the Cauchy-Schwarz inequality $|\langle\varphi|A|\psi\rangle|^2 \leqslant \langle\varphi|A|\varphi\rangle\langle\psi|A|\psi\rangle$, we arrive at the further estimate

$$\begin{aligned}
&\geqslant x^2\langle\varphi|A|\varphi\rangle\langle\psi|C|\psi\rangle + y^2\langle\varphi|C|\varphi\rangle\langle\psi|A|\psi\rangle\\
&\quad - 2\,|x\,y|\sqrt{\langle\varphi|A|\varphi\rangle\langle\psi|A|\psi\rangle}\sqrt{\langle\varphi|C|\varphi\rangle\langle\psi|C|\psi\rangle}\\
&= (|x|\sqrt{\langle\varphi|A|\varphi\rangle\langle\psi|C|\psi\rangle} - |y|\sqrt{\langle\varphi|C|\varphi\rangle\langle\psi|A|\psi\rangle})^2\\
&\geqslant 0.
\end{aligned}$$

■

APPENDIX B: DERIVATION OF THE BOLTZMANN EQUATION FROM THE BOSE-HUBBARD HAMILTONIAN

We transcribe [12] to bosons and generalize to arbitrary (integer) spin quantum numbers. Notably, the determinants for fermions will be replaced by permanents for bosons in Eq. (B28) below, due to the switch from anticommutators to commutators. In addition, for this section we consider the straightforward generalization to $\mathbb{Z}^d$ as underlying lattice. The derivation is formally very similar to Ref. [12], but for the sake of self-consistency and reproducibility we provide the details.

We start from the Hamiltonian in Eq. (4) and assume as in Refs. [10–12] that the initial state is gauge invariant, invariant under translations, and quasifree. It is thus completely determined by the two-point function

$$\langle\hat{a}_\sigma(k)^*\hat{a}_\tau(\tilde{k})\rangle = \delta(k-\tilde{k})W_{\sigma\tau}(k,0), \quad \sigma,\tau \in S, \qquad \text{(B1)}$$

where $\langle\cdot\rangle$ denotes the average with respect to the initial state and $S \equiv \{-n,\ldots,n\}$ enumerates spin quantum numbers. Averages of the form $\langle(a^*)^m a^n\rangle$ vanish unless $m = n$, and all other moments are determined by the Wick pairing rule. As discussed in Ref. [12], the quasifree property is approximately maintained up to times of order λ^{-2} for small $\lambda \ll 1$.

The true two-point function W_λ is defined via the relation $\delta(k-\tilde{k})W_\lambda(k,t)_{\sigma\tau} = \langle\hat{a}_\sigma(k,t)^*\hat{a}_\tau(\tilde{k},t)\rangle$; we expand W_λ for fixed t up to order λ^2,

$$W_\lambda(k,t) = W^{(0)}(k) + \lambda W^{(1)}(k,t) + \lambda^2 W^{(2)}(k,t) + \mathcal{O}(\lambda^3), \tag{B2}$$

and extract the collision operator from $W^{(2)}$, as in Ref. [12]. To emphasize independence of a specific spin basis, we consider $\langle \mathrm{f}, W_\lambda(k,t)\mathrm{g}\rangle$ for arbitrary vectors $\mathrm{f},\mathrm{g} \in \mathbb{C}^{2n+1}$. Here, $\langle\cdot,\cdot\rangle$ denotes the inner product in spin space, with the convention that the left argument is antilinear. We will use the vector valued operators

$$\hat{a}_{\mathrm{f}}(k)^* = \sum_{\sigma\in S} \bar{\mathrm{f}}_\sigma\, \hat{a}_\sigma(k)^*\, \mathfrak{e}_\sigma \quad \text{and} \quad \hat{a}_{\mathrm{g}}(k) = \sum_{\sigma\in S} \mathrm{g}_\sigma\, \hat{a}_\sigma(k)\, \mathfrak{e}_\sigma, \tag{B3}$$

where $\bar{\mathrm{f}}$ denotes the complex conjugate, $\mathrm{f}_\sigma,\mathrm{g}_\sigma$, $\sigma \in S$ denote the components of f and g and $\mathfrak{e}_\sigma$ enumerates the standard basis. The following operations map two $(2n+1)$-vector valued operators to a scalar-valued one:

$$v \odot w = \sum_{\sigma,\tau\in S} v_\sigma w_\tau \quad \text{and} \quad v\cdot w = \sum_{\sigma\in S} v_\sigma w_\sigma. \tag{B4}$$

For example,

$$\langle \hat{a}_{\mathrm{f}}(k,t)^* \odot \hat{a}_{\mathrm{g}}(\tilde{k},t)\rangle = \delta(k-\tilde{k})\,\langle \mathrm{f}, W_\lambda(k,t)\mathrm{g}\rangle.$$

The time derivative of the basic $(2n+1)$-vector valued operator becomes

$$\begin{aligned}\frac{d}{dt}\hat{a}_{\mathrm{f}}(k,t)^\# &= i[\hat{H},\hat{a}_{\mathrm{f}}(k,t)^\#]\\ &= i[\hat{H}_0,\hat{a}_{\mathrm{f}}(k)^\#](t) + i\,\frac{\lambda}{2}\,[\hat{H}_1,\hat{a}_{\mathrm{f}}(k)^\#](t),\end{aligned} \tag{B5}$$

where # denotes either nothing or an adjoint, corresponding to an annihilation or creation operator, respectively. For the quadratic H_0, it follows directly from the commutation relations that

$$\begin{aligned}[\hat{H}_0,\hat{a}_{\mathrm{g}}(k)] &= \int_{\mathbb{T}^d} dk'\,\omega(k')[\hat{a}(k')^*\cdot\hat{a}(k'),\hat{a}_{\mathrm{g}}(k)]\\ &= -\omega(k)\,\hat{a}_{\mathrm{g}}(k)\end{aligned} \tag{B6}$$

and, for the creation operator,

$$[\hat{H}_0,\hat{a}_{\mathrm{f}}(k)^*] = -[H_0,\hat{a}_{\mathrm{f}}(k)]^* = \omega(k)\,\hat{a}_{\mathrm{f}}(k)^*. \tag{B7}$$

For H_1, we first consider

$$\begin{aligned}[H_1,a_{\mathrm{g}}(z)] &= \frac{1}{2}\sum_{x\in\mathbb{Z}^d} V(x-z)\big(a(x)^*\cdot a(x)\big)\,a_{\mathrm{g}}(z)\\ &\quad + \frac{1}{2}\sum_{x\in\mathbb{Z}} V(z-x)a_{\mathrm{g}}(z)\,\big(a(x)^*\cdot a(x)\big)\end{aligned} \tag{B8}$$

such that in momentum space,

$$\begin{aligned}[\hat{H}_1,\hat{a}_{\mathrm{g}}(k_1)] &= \sum_{z\in\mathbb{Z}^d}[H_1,a_{\mathrm{g}}(z)]e^{-2\pi i\,k_1\cdot z}\\ &= \frac{1}{2}\int_{\mathbb{T}^d} dk\hat{V}(k-k_1)\hat{a}_{\mathrm{g}}(k_1) - \int_{(\mathbb{T}^d)^3} dk_{234}\,\delta(\underline{k})\\ &\quad\times \hat{V}(k_3-k_4)\hat{a}_{\mathrm{g}}(k_2)\big(\hat{a}(k_3)^*\cdot\hat{a}(k_4)\big).\end{aligned} \tag{B9}$$

Thus one arrives at

$$\begin{aligned}\frac{d}{dt}\hat{a}_{\mathrm{g}}(k,t) &= i\,[\hat{H},\hat{a}_{\mathrm{g}}(k_1,t)]\\ &= -i\,\omega(k)\,\hat{a}_{\mathrm{g}}(k_1,t) + i\,\frac{\lambda}{2}\,V(0)\,\hat{a}_{\mathrm{g}}(k_1,t)\\ &\quad - i\,\lambda\int_{(\mathbb{T}^d)^3} dk_{234}\,\delta(\underline{k})\,\hat{V}(k_3-k_4)\\ &\quad\times \hat{a}_{\mathrm{g}}(k_2,t)\,\big(\hat{a}(k_3,t)^*\cdot\hat{a}(k_4,t)\big),\end{aligned} \tag{B10}$$

where $\underline{k} = k_1 - k_2 + k_3 - k_4$. For the subsequent calculations, we use the notation $k_{1234} = (k_1,k_2,k_3,k_4)$ and introduce the following terms:

$$\begin{aligned}\mathcal{A}[h,a,b,c](k_1,t) &= \int_{(\mathbb{T}^d)^3} dk_{234}\,\delta(\underline{k})\,h(k_{1234},t)\\ &\quad\times \hat{V}(k_3-k_4)\,a(k_2,t)\,\big(b(k_3,t)\cdot c(k_4,t)\big)\end{aligned} \tag{B11}$$

and

$$\begin{aligned}\mathcal{A}_*[\bar{h},a,b,c](k_1,t) &= \int_{(\mathbb{T}^d)^3} dk_{234}\,\delta(\underline{k})\,\bar{h}(k_{1234},t)\\ &\quad\times \hat{V}(k_2-k_3)\,\big(a(k_2,t)\cdot b(k_3,t)\big)\,c(k_4,t),\end{aligned} \tag{B12}$$

where h is any complex-valued function and a,b,c are $(2n+1)$-component vector-valued operators as in Eq. (B3). Then $\mathcal{A}$ and $\mathcal{A}_*$ are again vector-valued operators and satisfy the relation

$$\big(\mathcal{A}[h,a,b^*,c](k,t)\big)^* = \mathcal{A}_*[\bar{h},c^*,b,a^*](k,t). \tag{B13}$$

The evolution equation (B10) can then be written as

$$\begin{aligned}\frac{d}{dt}\hat{a}_{\mathrm{g}}(k,t) &= -i\Big(\omega(k) - \frac{1}{2}\lambda\,V(0)\Big)\,\hat{a}_{\mathrm{g}}(k,t)\\ &\quad - i\lambda\,\mathcal{A}[id,\hat{a}_{\mathrm{g}},\hat{a}^*,\hat{a}](k,t),\end{aligned} \tag{B14}$$

and correspondingly, for the creation operator,

$$\begin{aligned}\Big(\frac{d}{dt}\hat{a}_{\mathrm{f}}(k,t)\Big)^* &= \frac{d}{dt}\hat{a}_{\mathrm{f}}(k,t)^*\\ &= i\Big(\omega(k) - \frac{1}{2}\lambda\,V(0)\Big)\,\hat{a}_{\mathrm{f}}(k,t)^*\\ &\quad + i\lambda\,\mathcal{A}_*[id,\hat{a}^*,\hat{a},\hat{a}_{\mathrm{f}}^*](k,t).\end{aligned} \tag{B15}$$

The linear part can be removed by defining

$$\mathfrak{a}_{\mathrm{g}}(k,t) = e^{i(\omega(k)-\frac{1}{2}\lambda V(0))t}\,\hat{a}_{\mathrm{g}}(k,t). \tag{B16}$$

The phase factor cancels in the correlator, such that

$$\langle \mathfrak{a}_{\mathrm{f}}(k,t)^* \odot \mathfrak{a}_{\mathrm{g}}(\tilde{k},t)\rangle = \langle \hat{a}_{\mathrm{f}}(k,t)^* \odot \hat{a}_{\mathrm{g}}(\tilde{k},t)\rangle. \tag{B17}$$

With the notation

$$\omega_{abcd} = \omega(k_a) - \omega(k_b) + \omega(k_c) - \omega(k_d), \tag{B18}$$

one finally arrives at

$$\frac{d}{dt}\mathfrak{a}_{\mathrm{g}}(k_1,t) = -i\lambda\,\mathcal{A}[e^{i\omega_{1234}t},\mathfrak{a}_{\mathrm{g}},\mathfrak{a}^*,\mathfrak{a}](k_1,t), \tag{B19}$$

and for the adjoint,

$$\frac{d}{dt}\mathfrak{a}_{\mathrm{f}}(k_1,t)^* = i\lambda\,\mathcal{A}_*[e^{-i\omega_{1234}t},\mathfrak{a}^*,\mathfrak{a},\mathfrak{a}_{\mathrm{f}}^*](k_1,t). \quad (B20)$$

Integrating Eq. (B19) leads to

$$\mathfrak{a}_{\mathrm{g}}(k_1,t) = \mathfrak{a}_{\mathrm{g}}(k_1,0) - i\lambda\int_0^t ds\,\mathcal{A}[e^{i\omega_{1234}s},\mathfrak{a}_{\mathrm{g}},\mathfrak{a}^*,\mathfrak{a}](k_1,s). \quad (B21)$$

We now iterate Eq. (B19) twice up to second order of the Dyson expansion, such that with an error of order λ^3,

$$\begin{aligned}\frac{d}{dt}\mathfrak{a}_{\mathrm{g}}(k_1,t) &= -i\lambda\,\mathcal{A}[e^{i\omega_{1234}t},\hat{a}_{\mathrm{g}},\hat{a}^*,\hat{a}](k_1,0)\\ &\quad -\lambda^2\int_0^t ds\,\mathcal{A}[e^{i\omega_{1234}t},\mathcal{A}[e^{i\omega_{2678}s},\hat{a}_{\mathrm{g}},\hat{a}^*,\hat{a}],\hat{a}^*,\hat{a}](k_1,s)\\ &\quad +\lambda^2\int_0^t ds\,\mathcal{A}[e^{i\omega_{1234}t},\hat{a}_{\mathrm{g}},\mathcal{A}^*[e^{-i\omega_{3678}s},\hat{a}^*,\hat{a},\hat{a}^*],\hat{a}](k_1,s)\\ &\quad -\lambda^2\int_0^t ds\,\mathcal{A}[e^{i\omega_{1234}t},\hat{a}_{\mathrm{g}},\hat{a}^*,\mathcal{A}[e^{i\omega_{4678}s},\hat{a},\hat{a}^*,\hat{a}]](k_1,s)\\ &= \lambda\frac{d}{dt}\mathfrak{a}_{\mathrm{g}}^{(1)}(k_1,t) + \lambda^2\frac{d}{dt}\mathfrak{a}_{\mathrm{g}}^{(2)}(k_1,t) + \mathcal{O}(\lambda^3). \end{aligned} \quad (B22)$$

We have thus obtained the expansion in λ (for fixed t):

$$\mathfrak{a}_{\mathrm{g}}(k_1,t) = \mathfrak{a}_{\mathrm{g}}^{(0)}(k_1,t) + \lambda\,\mathfrak{a}_{\mathrm{g}}^{(1)}(k_1,t) + \lambda^2\,\mathfrak{a}_{\mathrm{g}}^{(2)}(k_1,t) + \mathcal{O}(\lambda^3), \quad (B23)$$

where $\mathfrak{a}_{\mathrm{g}}^{(0)}(k,t) = \mathfrak{a}_{\mathrm{g}}^{(0)}(k,0) = \hat{a}_{\mathrm{g}}(k)$. A corresponding expression is satisfied by $\mathfrak{a}_{\mathrm{f}}(k,t)^*$. Iterating further yields the formal expansion

$$\begin{aligned}&\frac{d}{dt}\langle\mathfrak{a}_{\mathrm{f}}(k,t)^*\odot\mathfrak{a}_{\mathrm{g}}(\tilde{k},t)\rangle\\ &\quad = \sum_{n=0}^{\infty}\lambda^n\sum_{m=0}^{n}\frac{d}{dt}\langle\mathfrak{a}_{\mathrm{f}}(k,t)^{*(m)}\odot\mathfrak{a}_{\mathrm{g}}(\tilde{k},t)^{(n-m)}\rangle.\end{aligned} \quad (B24)$$

Therefore $W_\lambda(k,t)$ can be written as

$$\begin{aligned}&\delta(k-\tilde{k})\,\langle \mathrm{f},\,W_\lambda(k,t)\mathrm{g}\rangle\\ &\quad = \langle\mathfrak{a}_{\mathrm{f}}(k,0)^*\odot\mathfrak{a}_{\mathrm{g}}(\tilde{k},0)\rangle\\ &\qquad + \sum_{n=1}^{\infty}\lambda^n\int_0^t ds\sum_{m=0}^{n}\frac{d}{ds}\langle\mathfrak{a}_{\mathrm{f}}(k,s)^{*(m)}\odot\mathfrak{a}_{\mathrm{g}}(\tilde{k},s)^{(n-m)}\rangle\\ &\quad = \delta(k-\tilde{k})\sum_{n=0}^{\infty}\lambda^n\langle \mathrm{f},\,W^{(n)}(k,t)\mathrm{g}\rangle.\end{aligned} \quad (B25)$$

The zeroth order term of Eq. (B25) reads

$$\begin{aligned}\delta(k-\tilde{k})\,\langle \mathrm{f},\,W^{(0)}(k)\mathrm{g}\rangle &= \langle\mathfrak{a}_{\mathrm{f}}(k,0)^*\odot\mathfrak{a}_{\mathrm{g}}(\tilde{k},0)\rangle\\ &= \langle\hat{a}_{\mathrm{f}}(k)^*\odot\hat{a}_{\mathrm{g}}(\tilde{k})\rangle.\end{aligned} \quad (B26)$$

In the next two sections, we compute the first- and second-order terms.

1. First-order terms

We represent the various summands of the $W^{(1)}(k,t)$ term in Eq. (B25) as Feynman diagrams, which coincide for fermions and bosons. The first-order terms are determined by

$$\begin{aligned}&\delta(k_1-k_5)\langle \mathrm{f},\,W^{(1)}(k_1,t)\mathrm{g}\rangle\\ &\quad = i\int_0^t ds\,\langle\mathcal{A}_*[e^{-i\omega_{1234}s},\mathfrak{a}^*,\mathfrak{a},\mathfrak{a}_{\mathrm{f}}^*](k_1)\odot\mathfrak{a}_{\mathrm{g}}(k_5,s)^{(0)}\rangle\\ &\qquad - i\int_0^t ds\,\langle\mathfrak{a}_{\mathrm{f}}(k_1,s)^{*(0)}\odot\mathcal{A}[e^{i\omega_{5234}s},\mathfrak{a}_{\mathrm{g}},\mathfrak{a}^*,\mathfrak{a}](k_5)\rangle\\ &\quad = i\int_0^t ds\int_{(\mathbb{T}^d)^3}dk_{234}\,\delta(\underline{k})\,\hat{V}(k_2-k_3)\,e^{-i\omega_{1234}s}\\ &\qquad \times\big\langle\big(\hat{a}(k_2)^*\cdot\hat{a}(k_3)\big)\big(\hat{a}_{\mathrm{f}}(k_4)^*\odot\hat{a}_{\mathrm{g}}(k_5)\big)\big\rangle\\ &\qquad - i\int_0^t ds\int_{(\mathbb{T}^d)^3}dk_{234}\,\delta(\underline{k})\,\hat{V}(k_3-k_4)\,e^{i\omega_{5234}s}\\ &\qquad \times\big\langle\big(\hat{a}_{\mathrm{f}}(k_1)^*\odot\hat{a}_{\mathrm{g}}(k_2)\big)\big(\hat{a}(k_3)^*\cdot\hat{a}(k_4)\big)\big\rangle.\end{aligned} \quad (B27)$$

The first term is represented by the left graph in Fig. 7, as explained in detail in Ref. [12], where the corresponding Feynman rules are also listed. As last step, the average $\langle\cdot\rangle$ of the product of creation and annihilation operators at the

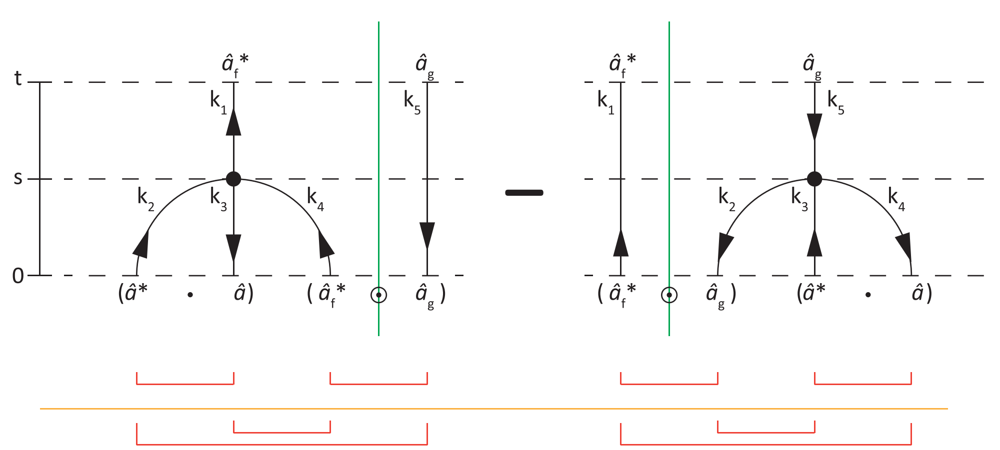

FIG. 7. (Color online) The diagrams of the first-order terms in λ.

bottom of the graph needs to be taken. Every $(\hat{a}(k_i)^* \cdot \hat{a}(k_j))$ entails a factor of $\hat{V}(k_i - k_j)$. By construction, if one starts to count the direction of the arrows from left to right in any of the time slices, they always start with an up-arrow and alternate from left to right in up-down combinations. This results in an alternating sequence of creation and annihilation operators at the bottom of the graph. The Wick pairings "⊔" shown under the graph follow from averaging this alternating sequence over the initial quasifree state. The average has a particularly simple form for the alternating order of creation and annihilation operators: it can then be computed according to the Wick rule:

$$\langle \hat{a}_{i_1}^* \hat{a}_{j_1} \cdots \hat{a}_{i_n}^* \hat{a}_{j_n} \rangle = \mathrm{perm}[K(i_k, j_l)]_{1 \leqslant k,l \leqslant n}, \tag{B28}$$

where

$$K(i_k, j_l) = \begin{cases} \langle \hat{a}_{i_k}^* \hat{a}_{j_l} \rangle & \text{if } k \leqslant l, \\ \langle \hat{a}_{j_l} \hat{a}_{i_k}^* \rangle & \text{if } k > l, \end{cases} \tag{B29}$$

and "perm" denotes the permanent of a matrix. For example, the expectation value $\langle \cdot \rangle$ over the initial state in the first term in Eq. (B27) can be expressed as

$$\begin{aligned}
&\big\langle (\hat{a}(k_2)^* \cdot \hat{a}(k_3)) (\hat{a}_\mathrm{f}(k_4)^* \odot \hat{a}_\mathrm{g}(k_5)) \big\rangle \\
&= \sum_{\sigma_1,\sigma,\tau \in S} \bar{\mathrm{f}}_\sigma \mathrm{g}_\tau \langle \hat{a}_{\sigma_1}(k_2)^* \hat{a}_{\sigma_1}(k_3) \hat{a}_\sigma(k_4)^* \hat{a}_\tau(k_5) \rangle \\
&= \sum_{\sigma_1,\sigma,\tau \in S} \bar{\mathrm{f}}_\sigma \mathrm{g}_\tau \mathrm{perm} \begin{bmatrix} \langle \hat{a}_{\sigma_1}(k_2)^* \hat{a}_{\sigma_1}(k_3) \rangle & \langle \hat{a}_{\sigma_1}(k_2)^* \hat{a}_\tau(k_5) \rangle \\ -\langle \hat{a}_{\sigma_1}(k_3) \hat{a}_\sigma(k_4)^* \rangle & \langle \hat{a}_\sigma(k_4)^* \hat{a}_\tau(k_5) \rangle \end{bmatrix} \\
&= \sum_{\sigma_1,\sigma,\tau \in S} \bar{\mathrm{f}}_\sigma \mathrm{g}_\tau \big(\langle \hat{a}_{\sigma_1}(k_2)^* \hat{a}_{\sigma_1}(k_3) \rangle \langle \hat{a}_\sigma(k_4)^* \hat{a}_\tau(k_5) \rangle \\
&\quad + \langle \hat{a}_{\sigma_1}(k_3) \hat{a}_\sigma(k_4)^* \rangle \langle \hat{a}_{\sigma_1}(k_2)^* \hat{a}_\tau(k_5) \rangle \big).
\end{aligned} \tag{B30}$$

The two Wick pairings shown in Fig. 7 represent the two different pairings in Eq. (B30). Since for instance, $\langle \hat{a}_{\sigma_1}(k_3) \hat{a}_\sigma(k_4)^* \rangle = \delta(k_3 - k_4) \tilde{W}(k_4)_{\sigma\sigma_1}$, the left diagram yields

$$\begin{aligned}
&\int_0^t ds\, \langle \dot{\mathfrak{a}}_\mathrm{f}(k_1,s)^{*(1)} \odot \mathfrak{a}_\mathrm{g}(k_5,s)^{(0)} \rangle \\
&\quad = it\, \delta(k_1 - k_5) \int_{\mathbb{T}^d} dk_2 (\hat{V}(0)\, \mathrm{tr}[W_2] \langle \mathrm{f}, W_1 \mathrm{g} \rangle \\
&\qquad + \hat{V}(k_1 - k_2) \langle \mathrm{f}, \tilde{W}_2 W_1 \mathrm{g} \rangle),
\end{aligned} \tag{B31}$$

where $\dot{\mathfrak{a}}(k,t) = \frac{d}{dt} \mathfrak{a}(k,t)$. The contribution of the right diagram in Fig. 7 can also be computed directly by taking an adjoint of the result above. When summing the two diagrams, the integrand containing $\hat{V}(0)$ cancels, and thus the first-order term is given by

$$\begin{aligned}
&W^{(1)}(k_1,t) = -it[R[W]_1, W_1], \\
&R[W]_1 = \int_{\mathbb{T}^d} dk\, \hat{V}(k_1 - k)\, W(k) \in \mathbb{C}_{(2n+1)\times(2n+1)}.
\end{aligned} \tag{B32}$$

All four diagrams in Fig. 7 have an interaction with zero momentum transfer (for instance, using the top left pairing leads to $k_4 = k_1$). Such diagrams will also appear in the second order and we call them *zero momentum transfer diagrams*.

2. Second-order terms

We next consider the second-order term in λ, which we decompose into a sum of four terms, obtained by evaluating the time-derivative in the equality

$$\begin{aligned}
&\delta(k - \tilde{k}) \langle \mathrm{f}, W^{(2)}(k,t) \mathrm{g} \rangle \\
&\quad = \int_0^t ds \sum_{m=0}^{2} \frac{d}{ds} \langle \mathfrak{a}_\mathrm{f}(k,s)^{*(m)} \odot \mathfrak{a}_\mathrm{g}(\tilde{k},s)^{(2-m)} \rangle.
\end{aligned} \tag{B33}$$

a. (1′,1) term

In the previous section, we have already shown that

$$\begin{aligned}
&\int_0^t ds\, \langle \dot{\mathfrak{a}}_\mathrm{f}(k_1,s)^{*(1)} \odot \mathfrak{a}_\mathrm{g}(k_5,s)^{(1)} \rangle \\
&\quad = \int_0^t ds_2 \int_0^{s_2} ds_1\, \langle \mathcal{A}^*[e^{-i\omega_{1234}s_2}, \mathfrak{a}^*, \mathfrak{a}, \mathfrak{a}_\mathrm{f}^*](k_1) \\
&\qquad \odot \mathcal{A}[e^{i\omega_{5678}s_1}, \mathfrak{a}_\mathrm{g}, \mathfrak{a}^*, \mathfrak{a}](k_5) \rangle,
\end{aligned} \tag{B34}$$

which can be represented by the Feynman diagram (Fig. 2 in Ref. [12]). In order to evaluate the diagram, we start with

$$\begin{aligned}
&\big\langle (a(k_2)^* \cdot a(k_3)) (a_\mathrm{f}(k_4)^* \odot a_\mathrm{g}(k_6)) (a(k_7)^* \cdot a(k_8)) \big\rangle \\
&\quad = \sum_{\sigma,\tau,\mu_1,\mu_2} \bar{\mathrm{f}}_\sigma \mathrm{g}_\tau \langle a_{\mu_1}(k_2)^*\, a_{\mu_1}(k_3) \\
&\qquad \times a_\sigma(k_4)^*\, a_\tau(k_6)\, a_{\mu_2}(k_7)^*\, a_{\mu_2}(k_8) \rangle.
\end{aligned} \tag{B35}$$

Using Eq. (C7) in Appendix C,

$$\begin{aligned}
&\langle \hat{a}_{s_1}(i_1)^*\, \hat{a}_{r_1}(j_1)\, \hat{a}_{s_2}(i_2)^*\, \hat{a}_{r_2}(j_2)\, \hat{a}_{s_3}(i_3)^*\, \hat{a}_{r_3}(j_3) \rangle \\
&= \mathrm{perm} \begin{bmatrix} \langle \hat{a}_{s_1}(i_1)^* \hat{a}_{r_1}(j_1) \rangle & \langle \hat{a}_{s_1}(i_1)^* \hat{a}_{r_2}(j_2) \rangle & \langle \hat{a}_{s_1}(i_1)^* \hat{a}_{r_3}(j_3) \rangle \\ \langle \hat{a}_{r_1}(j_1) \hat{a}_{s_2}(i_2)^* \rangle & \langle \hat{a}_{s_2}(i_2)^* \hat{a}_{r_2}(j_2) \rangle & \langle \hat{a}_{s_2}(i_2)^* \hat{a}_{r_3}(j_3) \rangle \\ \langle \hat{a}_{r_1}(j_1) \hat{a}_{s_3}(i_3)^* \rangle & \langle \hat{a}_{r_2}(j_2) \hat{a}_{s_3}(i_3)^* \rangle & \langle \hat{a}_{s_3}(i_3)^* \hat{a}_{r_3}(j_3) \rangle \end{bmatrix},
\end{aligned} \tag{B36}$$

one arrives at

$$\begin{aligned}
&\big\langle (a(k_2)^* \cdot a(k_3)) (a_\mathrm{f}(k_4)^* \odot a_\mathrm{g}(k_6)) (a(k_7)^* \cdot a(k_8)) \big\rangle \\
&\quad = \delta(k_3 - k_7)\delta(k_4 - k_6)\delta(k_2 - k_8) \langle \mathrm{f}, W_4 \mathrm{tr}[\tilde{W}_3 W_2] \mathrm{g} \rangle \\
&\qquad + \delta(k_2 - k_6)\delta(k_4 - k_8)\delta(k_3 - k_7) \langle \mathrm{f}, W_4 \tilde{W}_3 W_2 \mathrm{g} \rangle \\
&\qquad + \delta(k_2 - k_3)\delta(k_4 - k_6)\delta(k_7 - k_8) \langle \mathrm{f}, W_4 \mathrm{tr}[W_2] \mathrm{tr}[W_7] \mathrm{g} \rangle \\
&\qquad + \delta(k_2 - k_8)\delta(k_3 - k_4)\delta(k_6 - k_7) \langle \mathrm{f}, \tilde{W}_4 W_2 \tilde{W}_6 \mathrm{g} \rangle \\
&\qquad + \delta(k_6 - k_7)\delta(k_4 - k_8)\delta(k_2 - k_3) \langle \mathrm{f}, W_4 \tilde{W}_6 \mathrm{tr}[W_2] \mathrm{g} \rangle \\
&\qquad + \delta(k_7 - k_8)\delta(k_3 - k_4)\delta(k_2 - k_6) \langle \mathrm{f}, \tilde{W}_3 W_2 \mathrm{tr}[W_7] \mathrm{g} \rangle.
\end{aligned} \tag{B37}$$

Inserting this formula into (B34) yields the following expression for the $(1',1)$ term:

$$\begin{aligned}
&\int_0^t ds\, \langle \dot{\mathfrak{a}}_\mathrm{f}(k_1,s)^{*(1)} \odot \mathfrak{a}_\mathrm{g}(k_5,s)^{(1)} \rangle \\
&\quad = \delta(k_1 - k_5) \frac{1}{2} t^2 \langle \mathrm{f}, \mathcal{Z}[W]_1^{(1'1)} \mathrm{g} \rangle \\
&\qquad + \delta(k_1 - k_5) \int_0^t ds_2 \int_0^{s_2} ds_1 \int_{(\mathbb{T}^d)^3} dk_{234}\, \delta(\underline{k}) \\
&\qquad \times e^{-i\omega_{1234}(s_2 - s_1)} \langle \mathrm{f}, \mathcal{D}[W]_{234}^*\, \mathrm{g} \rangle.
\end{aligned} \tag{B38}$$

Here,

$$\mathcal{D}[W]^*_{234} = V(k_2-k_3)^2\, W_4\mathrm{tr}[\tilde{W}_3 W_2] + V(k_2-k_3)V(k_3-k_4)\, W_4\tilde{W}_3 W_2, \quad \text{(B39)}$$

resulting from the first two terms in Eq. (B37). Note the sign change compared to the fermionic case (see Eq. (62) in Ref. [12]). The remaining four terms all leads to a diagram with a zero momentum transfer and summing up their contribution yields

$$\mathcal{Z}[W]_1^{(1'1)} = \hat{V}(0)\{W_1, R[\tilde{W}]_1\}\,\mathrm{tr}[R] + R[\tilde{W}]_1\, W_1\, R[\tilde{W}]_1 + \hat{V}(0)^2\, W_1\,\mathrm{tr}[R]\mathrm{tr}[R]. \quad \text{(B40)}$$

b. (1,1′) term

By similar arguments, or taking the adjoint of the $(1',1)$ term, one arrives at

$$\int_0^t ds\, \langle \mathfrak{a}_{\mathrm{f}}(k_1,s)^{*(1)} \odot \dot{\mathfrak{a}}_{\mathrm{g}}(k_5,s)^{(1)}\rangle = \delta(k_1-k_5)\,\frac{1}{2}t^2 \langle \mathrm{f},\, \mathcal{Z}[W]_1^{(11')}\mathrm{g}\rangle + \delta(k_1-k_5)\int_0^t ds_2 \int_0^{s_2} ds_1 \int_{(\mathbb{T}^d)^3} dk_{234}\,\delta(\underline{k}) \times e^{i\omega_{1234}(s_2-s_1)}\langle \mathrm{f},\, \mathcal{D}[W]_{234}\mathrm{g}\rangle, \quad \text{(B41)}$$

where $\mathcal{Z}[W]_1^{(11')} = (\mathcal{Z}[W]_1^{(1'1)})^* = \mathcal{Z}[W]_1^{(1'1)}$ and

$$\mathcal{D}[W]_{234} = \hat{V}(k_2-k_3)^2\, W_4\mathrm{tr}[\tilde{W}_3 W_2] + \hat{V}(k_2-k_3)\hat{V}(k_3-k_4)\, W_4\tilde{W}_3 W_2, \quad \text{(B42)}$$

such that it hold $\mathcal{D}[W]^*_{234} = \mathcal{D}[W]_{234}$ by interchanging $k_2 \leftrightarrow k_4$ for the second term.

c. (2,0) term

The (2,0) term is given by the following expression:

$$\int_0^t ds\, \langle \dot{\mathfrak{a}}_{\mathrm{f}}(k_1,s)^{*(2)} \odot \mathfrak{a}_{\mathrm{g}}(k_5,s)^{(0)}\rangle = -\int_0^t ds_2 \int_0^{s_2} ds_1\, \langle \mathcal{A}_*[e^{-i\omega_{1234}s_2}, \mathcal{A}_*[e^{-i\omega_{2678}s_1}, \mathfrak{a}^*, \mathfrak{a}, \mathfrak{a}^*], \mathfrak{a}, \mathfrak{a}_{\mathrm{f}}^*](k_1) \odot \mathfrak{a}_{\mathrm{g}}(k_5)\rangle + \int_0^t ds_2 \int_0^{s_2} ds_1\, \langle \mathcal{A}_*[e^{-i\omega_{1234}s_2}, \mathfrak{a}^*, \mathcal{A}[e^{i\omega_{3678}s_1}, \mathfrak{a}, \mathfrak{a}^*, \mathfrak{a}], \mathfrak{a}_{\mathrm{f}}^*](k_1) \odot \mathfrak{a}_{\mathrm{g}}(k_5)\rangle - \int_0^t ds_2 \int_0^{s_2} ds_1\, \langle \mathcal{A}_*[e^{-i\omega_{1234}s_2}, \mathfrak{a}^*, \mathfrak{a}, \mathcal{A}_*[e^{-i\omega_{4678}s_1}, \mathfrak{a}^*, \mathfrak{a}, \mathfrak{a}_{\mathrm{f}}^*]](k_1) \odot \mathfrak{a}_{\mathrm{g}}(k_5)\rangle. \quad \text{(B43)}$$

To evaluate the contribution of the parings to the first term in Eq. (B43), we use

$$\Big\langle \big(a(k_6)^* \cdot a(k_7)\big)\big(a(k_8)^* \cdot a(k_3)\big)\big(a_{\mathrm{f}}(k_4)^* \odot a_{\mathrm{g}}(k_5)\big)\Big\rangle = \sum_{\sigma,\tau,\mu_1,\mu_2} \mathrm{f}_\sigma \mathrm{g}_\tau \big\langle a_{\mu_1}(k_6)^* a_{\mu_1}(k_7) a_{\mu_2}(k_8)^* \times a_{\mu_2}(k_3) a_\sigma(k_4)^* a_\tau(k_5)\big\rangle = \delta(k_7-k_4)\delta(k_8-k_3)\delta(k_6-k_5)\,\langle \mathrm{f},\, \tilde{W}_4 W_1 \mathrm{tr}[W_3]\mathrm{g}\rangle + \delta(k_6-k_3)\delta(k_8-\tilde{k})\delta(k_7-k_4)\,\langle \mathrm{f},\, \tilde{W}_4 W_3 W_1 \mathrm{g}\rangle + \text{zero momentum transfer diagrams.} \quad \text{(B44)}$$

The contributions of the second term in Eq. (B43) are

$$\Big\langle \big(a(k_2)^* \cdot a(k_6)\big)\big(a(k_7)^* \cdot a(k_8)\big)\big(a_{\mathrm{f}}(k_3)^* \odot a_{\mathrm{g}}(k_5)\big)\Big\rangle = \sum_{\sigma,\tau,\mu_1,\mu_2} \mathrm{f}_\sigma \mathrm{g}_\tau \big\langle a_{\mu_1}(k_2)^* a_{\mu_1}(k_6) a_{\mu_2}(k_7)^* \times a_{\mu_2}(k_8) a_\sigma(k_4)^* a_\tau(k_5)\big\rangle = \delta(k_8-k_4)\delta(k_7-\tilde{k})\delta(k_6-k_2)\,\langle \mathrm{f},\, \tilde{W}_4 W_1 \mathrm{tr}[W_2]\mathrm{g}\rangle + \delta(k_2-k_8)\delta(k_7-\tilde{k})\delta(k_6-k_4)\,\langle \mathrm{f},\, \tilde{W}_4 W_2 W_1 \mathrm{g}\rangle + \text{zero momentum transfer diagrams,} \quad \text{(B45)}$$

and the contributions of the third term (B43) are given by

$$\Big\langle \big(a(k_2)^* \cdot a(k_3)\big)\big(a(k_6)^* \cdot a(k_7)\big)\big(a_{\mathrm{f}}(k_8)^* \odot a_{\mathrm{g}}(k_5)\big)\Big\rangle = \sum_{\sigma,\tau,\mu_1,\mu_2} \mathrm{f}_\sigma \mathrm{g}_\tau \big\langle a_{\mu_1}(k_2)^* a_{\mu_1}(k_3) a_{\mu_2}(k_6)^* \times a_{\mu_2}(k_7) a_\sigma(k_8)^* a_\tau(k_5)\big\rangle = \delta(k_8-\tilde{k})\delta(k_3-k_6)\delta(k_2-k_7)\,\langle \mathrm{f},\, W_1 \mathrm{tr}[\tilde{W}_3 W_2]\mathrm{g}\rangle + \delta(k_2-k_7)\delta(k_6-\tilde{k})\delta(k_3-k_8)\,\langle \mathrm{f},\, \tilde{W}_3 W_2 W_1 \mathrm{g}\rangle + \text{zero momentum transfer diagrams.} \quad \text{(B46)}$$

Again, signs have changed as compared to the fermionic case. With the definitions

$$\mathcal{B}[W]^*_{1234} = \hat{V}(k_2-k_3)\hat{V}(k_3-k_4) \times (\tilde{W}_4 W_2 W_1 - \tilde{W}_4 W_3 W_1 - \tilde{W}_3 W_2 W_1) + V(k_2-k_3)^2(\tilde{W}_4 W_1 \mathrm{tr}[W_2] - \tilde{W}_4 W_1 \mathrm{tr}[W_3] - W_1 \mathrm{tr}[\tilde{W}_3 W_2]) \quad \text{(B47)}$$

and

$$\mathcal{Z}[W]_1^{(20)} = -\hat{V}(0)^2\, W_1\,\mathrm{tr}[R]\mathrm{tr}[R] - R[\tilde{W}]_1\, R[\tilde{W}]_1\, W_1 - \hat{V}(0)\, R[\tilde{W}]_1\, W_1\,\mathrm{tr}[R] - \hat{V}(0)\, R[\tilde{W}]_1\, W_1\,\mathrm{tr}[R], \quad \text{(B48)}$$

we obtain

$$\int_0^t ds\, \langle \dot{\mathfrak{a}}_{\mathrm{f}}(k_1,t)^{*(2)} \odot \mathfrak{a}_{\mathrm{g}}(k_5,t)^{(0)}\rangle = \delta(k_1-k_5)\frac{1}{2}t^2 \langle \mathrm{f},\, \mathcal{Z}[W]_1^{(20)}\mathrm{g}\rangle + \delta(k_1-k_5)\int_0^t ds_1 \int_0^{s_1} ds_2 \int_{(\mathbb{T}^d)^3} dk_{234}\,\delta(\underline{k}) \times e^{-i\omega_{1234}(s_2-s_1)}\langle \mathrm{f},\, \mathcal{B}[W]^*_{1234}\,\mathrm{g}\rangle. \quad \text{(B49)}$$

d. (0,2) term

Analogous to the (2,0) term, one arrives at

$$\int_0^t ds\, \langle \mathfrak{a}_{\mathrm{f}}(k_1,s)^{*(0)} \odot \dot{\mathfrak{a}}_{\mathrm{g}}(k_5,s)^{(2)}\rangle$$
$$= \delta(k_1-k_5)\,\frac{1}{2}t^2\,\langle \mathrm{f},\, \mathcal{Z}[W]^{(02)}\mathrm{g}\rangle$$
$$+\delta(k_1-k_5)\int_0^t ds_2\int_0^{s_2} ds_1\int_{(\mathbb{T}^d)^3} d^3k_{234}\,\delta(\underline{k})$$
$$\times\, e^{i\omega_{1234}(s_2-s_1)}\langle \mathrm{f},\, \mathcal{B}[W]_{1234}\,\mathrm{g}\rangle\,. \tag{B50}$$

3. The limit $\lambda \to 0$, $t = \mathcal{O}(\lambda^{-2})$

To summarize all second-order diagrams, we define

$$\mathcal{A}[W]_{1234} = \mathcal{D}[W]_{234} + \mathcal{B}[W]_{1234}, \tag{B51}$$

$$\mathcal{A}[W]^*_{1234} = \mathcal{D}[W]^*_{234} + \mathcal{B}[W]^*_{1234}, \tag{B52}$$

and using the identity

$$-[R[W]_1,\,[R[W]_1,\,W_1]]$$
$$= \mathcal{Z}[W]_1^{(1'1)} + \mathcal{Z}[W]_1^{(11')} + \mathcal{Z}[W]_1^{(20)} + \mathcal{Z}[W]_1^{(02)}, \tag{B53}$$

one finds that

$$\int_0^t ds\,\frac{d}{ds}\sum_{m=0}^{2}\langle \mathfrak{a}_{\mathrm{f}}(k_1,s)^{*(m)} \odot \mathfrak{a}_{\mathrm{g}}(k_5,s)^{(2-m)}\rangle$$
$$= -\delta(k_1-k_5)\,\frac{1}{2}t^2\,\langle \mathrm{f},\,[R[W]_1,\,[R[W]_1,\,W_1]]\mathrm{g}\rangle$$
$$+\delta(k_1-k_5)\int_0^t ds_1\int_0^{s_1} ds_2\int_{(\mathbb{T}^d)^3} dk_{234}\,\delta(\underline{k})$$
$$\times\, e^{i\omega_{1234}(s_2-s_1)}\langle \mathrm{f},\,\mathcal{A}[W]_{1234}\,\mathrm{g}\rangle$$
$$+\,\delta(k_1-k_5)\int_0^t ds_1\int_0^{s_1} ds_2\int_{(\mathbb{T}^d)^3} dk_{234}\,\delta(\underline{k})$$
$$\times\, e^{-i\omega_{1234}(s_2-s_1)}\langle \mathrm{f},\,\mathcal{A}[W]^*_{1234}\,\mathrm{g}\rangle. \tag{B54}$$

Hence the second-order term $W^{(2)}$ is given by

$$W^{(2)}(k_1,t) = W_{\mathrm{z}}^{(2)}(k_1,t) + W_{\mathrm{c}}^{(2)}(k_1,t), \tag{B55}$$

where

$$W_{\mathrm{z}}^{(2)}(k_1,t) = -\tfrac{1}{2}t^2\,[R[W]_1,\,[R[W]_1,\,W_1]] \tag{B56}$$

and

$$W_{\mathrm{c}}^{(2)}(k_1,t)$$
$$= \int_0^t ds_1\int_0^{s_1} ds_2\int_{(\mathbb{T}^d)^3} dk_{234}\,\delta(\underline{k})\big(e^{i\omega_{1234}(s_1-s_2)}\mathcal{A}[W]_{1234}$$
$$+\,e^{-i\omega_{1234}(s_1-s_2)}\mathcal{A}[W]^*_{1234}\big). \tag{B57}$$

The collision operator is determined by taking at second order the limit $\lambda \to 0$ and simultaneous long times $\lambda^{-2}t$ with t of order 1. More explicitly,

$$t\,\mathcal{C}[W^{(0)}](k) = \lim_{\lambda\to 0}\lambda^2\,W_{\mathrm{c}}^{(2)}(k,\lambda^{-2}t), \tag{B58}$$

where $W_{\mathrm{c}}^{(2)}$ is defined in Eq. (B57). To evaluate the limit, we make use of

$$\lim_{\lambda\to 0}\lambda^2\int_0^{\lambda^{-2}t} ds_1\int_0^{s_1} ds_2\, e^{\pm i\omega_{1234}(s_1-s_2)}$$
$$= t\int_0^{\infty} ds\, e^{\pm i\omega_{1234}s} = t\left(\pm i\,\mathcal{P}\left(\frac{1}{\omega_{1234}}\right) + \pi\,\delta(\omega_{1234})\right), \tag{B59}$$

where $\mathcal{P}$ denotes the principal value. This yields

$$\lim_{\lambda\to 0}\lambda^2\,W_{\mathrm{c}}^{(2)}(k,\lambda^{-2}\,t)$$
$$= t\,\pi\int_{(\mathbb{T}^d)^3} dk_{234}\,\delta(\underline{k})\,\delta(\omega_{1234})\langle \mathrm{f},\,(\mathcal{A}[W]_{1234}+\mathcal{A}[W]^*_{1234})\mathrm{g}\rangle$$
$$+\,i\,t\int_{(\mathbb{T}^d)^3} dk_{234}\,\delta(\underline{k})\,\mathcal{P}\left(\frac{1}{\omega_{1234}}\right)$$
$$\times\,\langle \mathrm{f},\,(\mathcal{A}[W]_{1234}-\mathcal{A}[W]^*_{1234})\mathrm{g}\rangle. \tag{B60}$$

We note that in case $W_{\sigma\tau}(k) = \delta_{\sigma\tau}W_\sigma(k)$ the term containing the principal part vanishes. The effective Hamiltonian results from the $(2n+1)$-fold degeneracy of the unperturbed H_0.

APPENDIX C: BOSONIC CORRELATIONS

1. Two-point function

Let $\mathsf{H} = \sum_{k,l\in\mathbb{Z}} H_{kl}\,a_k^* a_l$ be the second quantization of the one-particle matrix H. It is assumed that e^{-H} is trace class and $\det(1+e^H) \neq 0$. We use the identities

$$e^{-\mathsf{H}}a_i^* e^{\mathsf{H}} = \sum_{j\in\mathbb{Z}} a_j^*(e^{-H})_{ji}, \quad e^{-\mathsf{H}}a_i e^{\mathsf{H}} = \sum_{j\in\mathbb{Z}}(e^{H})_{ij}a_j. \tag{C1}$$

Then

$$\begin{aligned}\langle a_i^* a_j\rangle &= \frac{1}{Z}\mathrm{tr}[e^{-\mathsf{H}}a_i^* a_j]\\ &= \sum_n \frac{1}{Z}\mathrm{tr}[a_n^*(e^{-H})_{ni}e^{-\mathsf{H}}a_j]\\ &= \sum_n \frac{1}{Z}\mathrm{tr}[(e^{-H})_{ni}e^{-\mathsf{H}}a_j a_n^*]\\ &= \sum_n (e^{-H})_{ni}\frac{1}{Z}\mathrm{tr}[e^{-\mathsf{H}}a_j a_n^*]\\ &= \sum_n (e^{-H})_{ni}\frac{1}{Z}\mathrm{tr}[e^{-\mathsf{H}}(\delta_{nj}+a_n^* a_j)]\\ &= (e^{-H})_{ji} + \sum_n \langle a_n^* a_j\rangle(e^{-H})_{ni}\end{aligned} \tag{C2}$$

with the partition function $Z = \mathrm{tr}[e^{-\mathsf{H}}]$. Rearranging gives

$$\sum_{n\in\mathbb{Z}}\langle a_n^*(1-e^{-H})_{ni}a_j\rangle = (e^{-H})_{ji}. \tag{C3}$$

Finally, multiplying this expression by $(1-e^{-H})^{-1})_{im}$ and summing over the i variable, we obtain

$$\langle a_m^* a_j\rangle = \big((e^H-1)^{-1}\big)_{jm}. \tag{C4}$$

2. Expansion as permanent

We prove recursively that

$$\langle a_{i_1}^* a_{j_1} \cdots a_{i_n}^* a_{j_n} \rangle = \operatorname{perm}[K(i_k, j_l)]_{1 \leqslant k,l \leqslant n}, \tag{C5}$$

where

$$K(i_k, j_l) = \begin{cases} \langle a_{i_k}^* a_{j_l} \rangle & \text{if } k \leqslant l, \\ \langle a_{l_l} a_{i_k}^* \rangle & \text{if } k > l. \end{cases} \tag{C6}$$

For $n = 1$, the formula holds by definition. Suppose the formula (C5) has been established for some n, i.e.,

$$\langle a_{i_1}^* a_{j_1} \cdots a_{i_n}^* a_{j_n} \rangle = \operatorname{perm}\begin{bmatrix} \langle a_{i_1}^* a_{j_1} \rangle & \langle a_{i_1}^* a_{j_2} \rangle & \cdots & \langle a_{i_1}^* a_{j_n} \rangle \\ \langle a_{j_1} a_{i_2}^* \rangle & \langle a_{i_2}^* a_{j_2} \rangle & \cdots & \langle a_{i_2}^* a_{j_n} \rangle \\ \vdots & \vdots & \ddots & \vdots \\ \langle a_{j_1} a_{i_n}^* \rangle & \langle a_{j_2} a_{i_n}^* \rangle & \cdots & \langle a_{i_n}^* a_{j_n} \rangle \end{bmatrix}. \tag{C7}$$

We will need one more expression for $\langle \cdots \rangle$ such that in the first k pairs the annihilation operator precedes the creation operator,

$$\langle a_{j_1} a_{i_1}^* \cdots a_{j_k} a_{i_k}^* a_{i_{k+1}}^* a_{j_{k+1}} \cdots a_{i_n}^* a_{j_n} \rangle = \operatorname{perm}\begin{bmatrix} \langle a_{j_1}^* a_{i_1} \rangle & \cdots & \langle a_{i_1}^* a_{j_k} \rangle & \langle a_{i_1}^* a_{j_{k+1}} \rangle & \cdots & \langle a_{i_1}^* a_{j_n} \rangle \\ \vdots & \ddots & \vdots & \vdots & \ddots & \vdots \\ \langle a_{j_k} a_{i_1}^* \rangle & \cdots & \langle a_{j_k} a_{i_k}^* \rangle & \langle a_{i_k}^* a_{j_{k+1}} \rangle & \cdots & \langle a_{i_k}^* a_{j_n} \rangle \\ \langle a_{j_{k+1}} a_{i_1}^* \rangle & \cdots & \langle a_{j_{k+1}} a_{i_k}^* \rangle & \langle a_{i_{k+1}}^* a_{j_{k+1}} \rangle & \cdots & \langle a_{i_{k+1}}^* a_{j_n} \rangle \\ \vdots & \ddots & \vdots & \vdots & \ddots & \vdots \\ \langle a_{j_n} a_{i_1}^* \rangle & \cdots & \langle a_{j_n} a_{i_k}^* \rangle & \langle a_{j_n} a_{i_{k+1}}^* \rangle & \cdots & \langle a_{i_n}^* a_{j_n} \rangle \end{bmatrix}. \tag{C8}$$

Let us prove this formula. For $k = 0$, it agrees with (C7). Suppose it to be true for some k. Let us then prove that the formula (C8) holds for $k + 1$,

$$\begin{aligned} &\langle a_{j_1} a_{i_1}^* \cdots a_{j_{k+1}} a_{i_{k+1}}^* a_{i_{k+2}}^* a_{j_{k+2}} \cdots a_{i_n}^* a_{j_n} \rangle \\ &= \langle a_{j_1} a_{i_1}^* \cdots a_{j_k} a_{i_k}^* a_{i_{k+1}}^* a_{j_{k+1}} \cdots a_{i_n}^* a_{j_n} \rangle \\ &\quad + \delta_{i_{k+1}, j_{k+1}} \langle a_{j_1} a_{i_1}^* \cdots a_{j_k} a_{i_k}^* a_{i_{k+2}}^* a_{j_{k+2}} \cdots a_{i_n}^* a_{j_n} \rangle. \end{aligned} \tag{C9}$$

Using the expression (C8) and considering the expansion of the permanent in the $(k+1)^{\text{th}}$ column (or row), it is easy to see that (C9) corresponds to the expression (C8) but with the diagonal term $a_{i_{k+1}}^* a_{j_{k+1}}$ replaced by $a_{j_{k+1}} a_{i_{k+1}}^*$. Therefore (C8) holds for $k + 1$, too.

Now we prove (C7) for $n + 1$ by using (C7) for n and (C8) for n and $k \leqslant n$,

$$\begin{aligned} &\langle a_q^* a_{j_1} \cdots a_{i_{n+1}}^* a_{j_{n+1}} \rangle \\ &= \frac{1}{Z} \operatorname{tr}\big[e^{-\mathsf{H}} a_q^* a_{j_1} \cdots a_{i_{n+1}}^* a_{j_{n+1}}\big] \\ &= \sum_{n \in \mathbb{Z}} \frac{1}{Z} (e^{-H})_{mq} \operatorname{tr}\big[e^{-\mathsf{H}} a_{j_1} \cdots a_{i_{n+1}}^* a_{j_{n+1}} a_m^*\big] \\ &= \sum_{m \in \mathbb{Z}} (e^{-H})_{mq} \langle a_m^* a_{j_1} \cdots a_{i_{n+1}}^* a_{j_{n+1}} \rangle \\ &\quad + \sum_{p=2}^{n+1} (e^{-H})_{j_p q} \langle a_{j_1} a_{i_2}^* \cdots a_{j_{p-1}} a_{i_p}^* a_{i_{p+1}}^* a_{j_{p+1}} \cdots a_{i_{n+1}}^* a_{j_{n+1}} \rangle \\ &\quad + (e^{-H})_{j_1 q} \langle a_{i_2}^* a_{j_2} \cdots a_{i_{n+1}}^* a_{j_{n+1}} \rangle. \end{aligned}$$

We take the term with the sum over $m \in \mathbb{Z}$ together with the first one and multiply the whole expression by $\sum_{q \in \mathbb{Z}} ((1 - e^{-H})^{-1})_{q i_1}$ to obtain

$$\begin{aligned} &\langle a_{i_1}^* a_{j_1} \cdots a_{i_{n+1}}^* a_{j_{n+1}} \rangle \\ &= \langle a_{i_1}^* a_{j_1} \rangle \langle a_{i_2}^* a_{j_2} \cdots a_{i_{n+1}}^* a_{j_{n+1}} \rangle \\ &\quad + \sum_{p=2}^{n+1} \langle a_{i_1}^* a_{j_p} \rangle \langle a_{j_1} a_{i_2}^* \cdots a_{j_{p-1}} a_{i_p}^* a_{i_{p+1}}^* a_{j_{p+1}} \cdots a_{i_{n+1}}^* a_{j_{n+1}} \rangle. \end{aligned} \tag{C10}$$

Using (C7) and (C8) for n terms, we see that this last expression is nothing else than the expansion with respect to the first row of (C7) with n substituted by $n + 1$.

APPENDIX D: INITIAL WIGNER STATE $W(k,0)$

The initial Wigner state $W(k,0)$ used in the simulations (Fig. 1) has entries

$$W_{\uparrow\uparrow}(k,0) = \tfrac{3}{5}\,\Gamma\big(1 + \tfrac{1}{2}\cos\big(4\pi\big(k + \tfrac{1}{5}\big)\big)\big) + \tfrac{1}{5}, \tag{D1}$$

$$\begin{aligned} W_{00}(k,0) = &\tfrac{3}{20}\operatorname{erf}\big(\cos\big(2\pi\big(k + \tfrac{1}{5}\big)\big)\big) + \tfrac{1}{5} \\ &+ \tfrac{3}{5}\operatorname{atan}\big(\sin\big(2\pi\big(k + \tfrac{1}{5}\big) - \tfrac{1}{5}\big)\big) + \tfrac{3}{20}\pi, \end{aligned} \tag{D2}$$

$$W_{\downarrow\downarrow}(k,0) = \tfrac{3}{10}\, e^{-\cos(6\pi(k+1/5-\gamma))} + \tfrac{1}{20}, \tag{D3}$$

$$W_{\uparrow 0}(k,0) = \tfrac{3}{10}\sin\big(2\pi\big(k + \tfrac{1}{5}\big)\big), \tag{D4}$$

$$W_{\uparrow\downarrow}(k,0) = -\tfrac{1}{10}\, i\cos\big(6\pi\big(k - \tfrac{1}{20}\big)\big), \tag{D5}$$

$$W_{0\downarrow}(k,0) = \tfrac{3}{20}\sin(e^{-2\pi i(k+1/5)}), \tag{D6}$$

and the remaining off-diagonal entries are respective complex conjugates since $W(k,0)$ is Hermitian.

[1] I. Bloch, J. Dalibard, and W. Zwerger, Rev. Mod. Phys. **80**, 885 (2008).

[2] I. Bloch, J. Dalibard, and S. Nascimbène, Nat. Phys. **8**, 267 (2012).

[3] M. Greiner, O. Mandel, T. Esslinger, T. W. Hänsch, and I. Bloch, Nature (London) **415**, 39 (2002).

[4] A. A. Burkov, M. D. Lukin, and E. Demler, Phys. Rev. Lett. **98**, 200404 (2007).

[5] S. Hofferberth, I. Lesanovsky, B. Fischer, T. Schumm, and J. Schmiedmayer, Nature (London) **449**, 324 (2007).

[6] I. Bloch, Nature (London) **453**, 1016 (2008).

[7] T. Kinoshita, T. Wenger, and D. S. Weiss, Nature (London) **440**, 900 (2006).
[8] C. Kollath, A. M. Lauchli, and E. Altman, Phys. Rev. Lett. **98**, 180601 (2007).
[9] C. Trefzger and K. Sengupta, Phys. Rev. Lett. **106**, 095702 (2011).
[10] M. L. R. Furst, C. B. Mendl, and H. Spohn, Phys. Rev. E **86**, 031122 (2012).
[11] M. L. R. Furst, C. B. Mendl, and H. Spohn, Phys. Rev. E **88**, 012108 (2013).
[12] M. L. R. Fürst, J. Lukkarinen, P. Mei, and H. Spohn, J. Phys. A **46**, 485002 (2013).
[13] J. Lukkarinen, P. Mei, and H. Spohn, arXiv:1212.2575.
[14] M. Moeckel and S. Kehrein, Phys. Rev. Lett. **100**, 175702 (2008).
[15] M. Kollar, F. A. Wolf, and M. Eckstein, Phys. Rev. B **84**, 054304 (2011).
[16] M. Gring, M. Kuhnert, T. Langen, T. Kitagawa, B. Rauer, M. Schreitl, I. Mazets, D. Adu Smith, E. Demler, and J. Schmiedmayer, Science **337**, 1318 (2012).
[17] S. Braun, J. P. Ronzheimer, M. Schreiber, S. S. Hodgman, T. Rom, I. Bloch, and U. Schneider, Science **339**, 52 (2013).
[18] H. Spohn, Physica D **239**, 627 (2010).
[19] A. Rapp, S. Mandt, and A. Rosch, Phys. Rev. Lett. **105**, 220405 (2010).